ISSN 2538-1016; 60

NEW ZEALAND
DEPARTMENT OF SCIENTIFIC AND INDUSTRIAL RESEARCH

BULLETIN 208

INTERNAL STRUCTURE IN MARINE SHELF, SLOPE, AND ABYSSAL SEDIMENTS EAST OF NEW ZEALAND

by
H. M. PANTIN

New Zealand Oceanographic Institute

Memoir No. 60

1972

NEW ZEALAND
DEPARTMENT OF SCIENTIFIC AND INDUSTRIAL RESEARCH

BULLETIN 208

INTERNAL STRUCTURE IN MARINE SHELF, SLOPE, AND ABYSSAL SEDIMENTS EAST OF NEW ZEALAND

by
H. M. PANTIN

New Zealand Oceanographic Institute

Memoir No. 60

Wellington
1972

Price: NZ$2

New Zealand Department of Scientific and Industrial Research Bulletin 208

Received for publication December 1968

A. R. SHEARER, GOVERNMENT PRINTER, WELLINGTON, NEW ZEALAND—1972

FOREWORD

Recent opportunities of coring marine sediments deposited off the East Coast of the North Island have provided for the first time materials for study of sedimentation in this region.

In this memoir the author describes and classifies the sedimentary structures and the processes of transport and deposition that have given rise to them.

The material has been prepared for publication by Mrs R. J. Wanoa.

J. W. BRODIE, Director,
New Zealand Oceanographic Institute,
Wellington.

CONTENTS

FIGURES

TABLES

INTERNAL STRUCTURE IN MARINE SHELF, SLOPE, AND ABYSSAL SEDIMENTS EAST OF NEW ZEALAND

by H. M. PANTIN
Institute of Geological Sciences
Leeds, England

Abstract

A programme of core sampling was carried out in the Cape Palliser region to determine the nature of the sediments in the area and identify their various types of internal structure. Coring positions were chosen to cover shelf, slope, canyons, trench, and ocean basin. Stratigraphic diagrams of all cores investigated are given.

Shelf sediments grade outwards from sand to mud. On the slope and in the canyons, mud is dominant, *but pebbly mud, glauconitic sediments, silty turbidite beds, and thin* sand and silt layers also occur. The sand and silt components of the shelf, slope, and canyon sediments are dominantly terrigenous and non-volcanic: in bulk, they are medium to very pale grey. The mud component when dry varies from pale olive with an obvious chroma, to pale grey with no significant chroma.

The main trench sediment is hemipelagic mud, with Foraminifera in small but significant numbers. The sediment when dry is pale to very pale olive. Pale grey to white silty turbidites are also present in two cores, and the third has a superficial relatively thin layer of hemipelagic mud underlain by a thick layer of grey sand extending to the base of the core. The sand and silt components of the trench sediments are dominantly terrigenous and non-volcanic, but foraminifera make up an important minor component.

Both cores from the ocean basin consist of a relatively thick layer of pelagic foraminiferal mud, underlain by a band of rhyolitic pumiceous silt. The pelagic mud is pale to very pale sub-olive and the pumiceous silt is white. The latter may represent an eruption from the Taupo centre.

The mechanisms which may control transport and deposition of marine sediment (wave turbulence; turbidity effect; tidal currents; river outflow effect; ocean currents; storm drift currents; giant eddies; tsunami-generated currents) are classified as continuous, cyclic, variable, or discontinuous. Their probable relative importance in the Cape Palliser region is discussed.

The internal structure in the sediments may be considered as organic or inorganic; the characteristics of these two categories are classified and described. The relative abundance of the structures in the various bathymetric zones are tabulated, and references are given, where possible, to similar structures in unconsolidated or fossil sediments from other areas.

Experiments carried out on a series of olive and grey muds from shelf, slope, and canyon to elucidate the nature of the colour differences indicate that the colour of the olive mud is due to the presence of adsorbed organic compounds, probably pheophytins. These compounds are lacking in the grey muds. Similar experiments indicate that the colour difference between pale alteration burrows and the corresponding matrix is due to the removal of adsorbed organic matter from calcilutite particles, and of iron compounds from clay particles.

Alternative explanations are suggested for the absence of dark sulphide (miomelanosis) from pale alteration burrows where they penetrate anaerobic sulphide-bearing zones, artificially induced by the sealing up of core samples; one explanation involves the same assumptions as the preferred explanations for the colour change in pale alteration burrows.

INTRODUCTION

The sediments described lie mainly within an elongated area, covering about 3,100 square miles and extending eastwards from the neighbourhood of Cape Palliser to Sta. E9a and E9b (figs. 1 and 2).

Sta. E7 is at the southern apex of this area. The area includes part of the continental shelf at its westward end, crosses both the continental slope and the Hikurangi Trench, and reaches the Southwestern Pacific Basin (called the "ocean basin" in the following description). Four cores (A802, A805, E10a, and E10b) were taken in the Madden Depression, about 70 miles to the north of the main area, and another (A791) was taken in Palliser Bay, about 15 miles west of the main area.

Sampling was done with a piston corer with a 3.66 m barrel, internal diameter 5 cm. A short pilot corer was used as a trigger weight. Of the 35 piston cores obtained, 32 merited investigation.

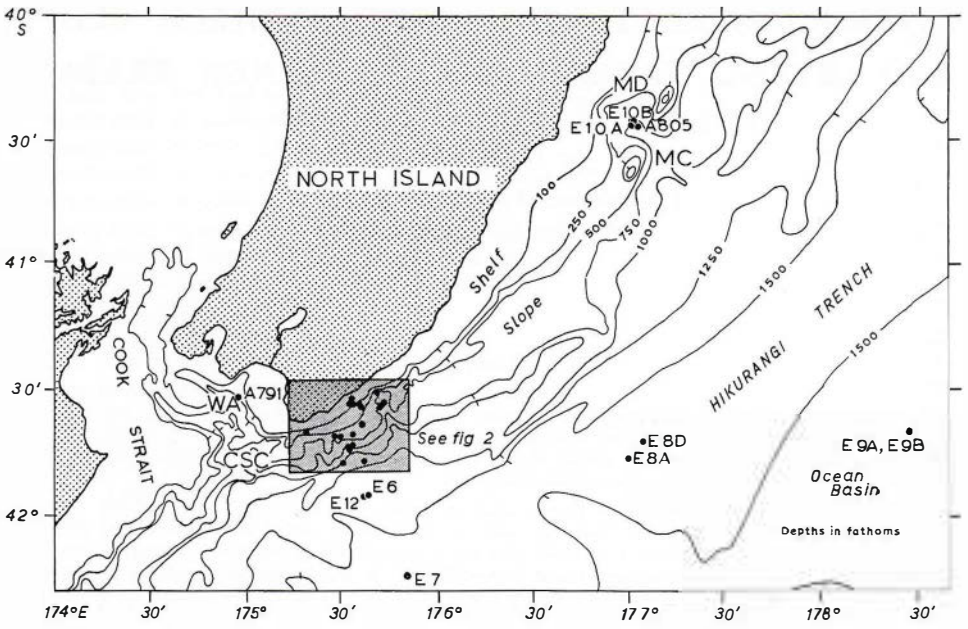

FIG. 1. Locality chart showing station positions. MD, Madden Depression; MC, Madden Canyon; CSC, Cook Strait Canyon; WA, Wairarapa Arm. The location of Cape Palliser is 41° 37′ S, 175° 16′ E. Detail of the Cape Palliser region (hatched area) is shown in Fig. 2.

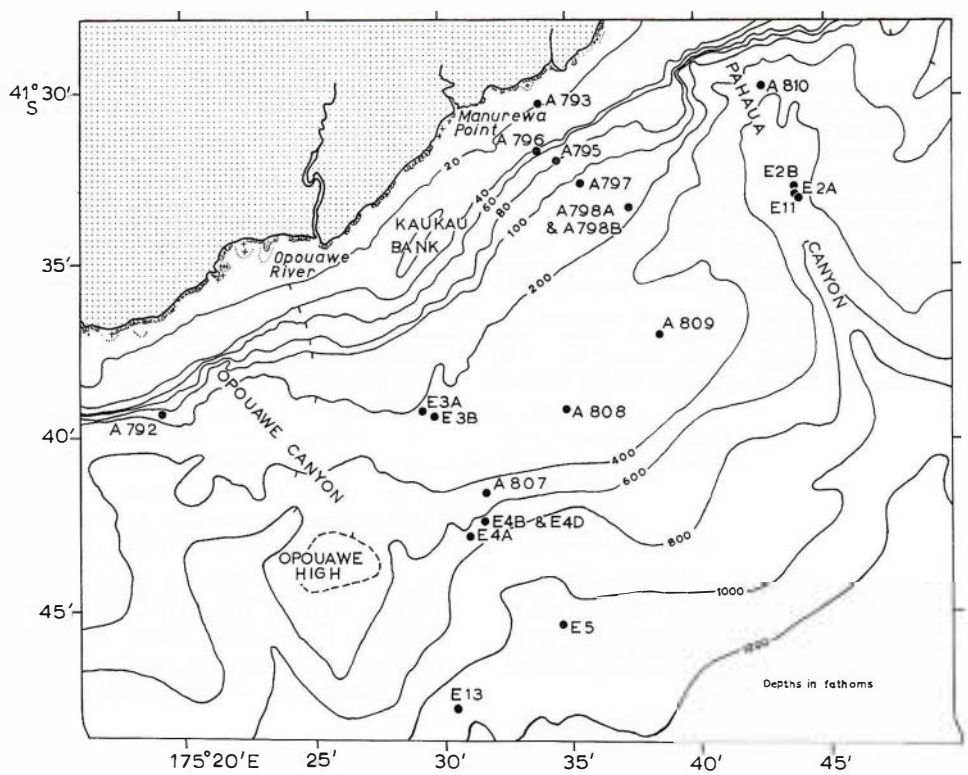

FIG. 2. Station positions east of Cape Palliser (Dashed isobath on Opouawe High is 500 fathoms).

Table 1. Station details

Sta. No.	*Bathymetric zone*	*Latitude* (° 'S)	*Longitude* (° 'E)	*Depth* (m)*
A793	Shelf	41 30.5	175 34.0	44
A795	"	41 32.0	175 34.6	154
A796	"	41 31.8	175 34.0	123
A792	Slope	41 39.5	175 19.5	296
A797	Top of slope	41 32.7	175 35.6	199
A798A	Slope	41 33.3	175 37.5	351
A798B	"	41 33.3	175 37.5	454
A807	"	41 41.7	175 32.0	914
A808	"	41 39.2	175 35.2	472
A809	"	41 37.0	175 38.8	472
E3A	"	41 39.3	175 29.6	439
E3B	"	41 39.3	175 30.0	476
E4A	"	41 42.9	175 31.4	1,298
E4B	"	41 42.5	175 32.0	1,207
E4D	"	41 42.5	175 32.0	1,207
E5	"	41 45.5	175 35.0	1,975
E6	"	41 55.0	175 40.0	2,579
E12	"	41 55.0	175 40.0	2,579
E13	"	41 46.9	175 34.0	2,085
A791	Canyon	41 27.5	174 58.3	560
A805	"	40 26.5	177 03.0	1,372
A810	"	41 29.8	175 42.5	933
E2A	"	41 33.0	175 44.0	1,298
E2B	"	41 33.7	175 44.0	1,298
E10A	"	40 26.5	177 01.5	1,353
E10B	"	40 26.0	177 02.0	1,353
E11	"	41 33.0	175 44.0	1,280
E7	Trench	42 13.0	175 50.0	2,750
E8A	"	41 45.0	177 00.0	2,790
E8D	"	41 40.5	177 04.0	2,800
E9A	Ocean basin	41 40.0	178 30.0	2,800
E9B	"	41 40.0	178 30.0	2,800

As the cores were collected at different times, some drift while on station will account for the different depths of A798A and A798B.

*1 fathom = 1.83 metres

These cores were collected on two cruises of m.v. *Taranui: the "A" series from 28.3.63 to 6.4.63,* and the "E" series from 14.8.63 to 19.8.63. Most of the cores were taken in pairs, at roughly the same locality. Structures in the cores were observed by cutting a longitudinal flat surface on each core with a scalpel or a wood-plane. The cores of series "A" were dry by the time this operation was performed; the cores of series "E" were still damp when first investigated, although some of the structures were not photographed until this series, too, had dried out.

The bathymetry of the area has been previously described (Brodie and Hatherton 1958; Pantin 1963). Station positions (table 1) were chosen to cover the main types of bathymetric environment in the area in order to elucidate the changes in sediment type from one environment to another and determine the principal varieties of internal structure found in these sediments.

The stratigraphy and lithology of the various cores are shown in the core diagrams (figs. 3–8). Some cores consisted throughout of relatively undisturbed sediment, while others had a relatively undisturbed upper portion underlain by a zone of highly distorted sediment sucked in by the piston during the coring process. These sucked-in portions have been omitted from most of the core diagrams. In the diagram of E2b, (fig. 6) however, the sucked-in portion has been shown, since one of the samples for chemical analysis was taken from this part of the core.

The core diagrams do not represent the actual thickness of sediment penetrated, as compaction (especially in the topmost metre or so of each core), and even sediment loss, are likely to occur. Because of the complex conditions controlling sediment compaction during and after core recovery it is not desirable to use a simplified correction factor, and the core diagrams presented here have *not* been corrected for possible vertical compaction of the sediment.

DESCRIPTION OF SEDIMENTS AND PROCESSES OF SEDIMENTATION

GENERAL NATURE OF THE SEDIMENTS

Although some of the coring stations are widely separated, the cores give a clear picture of the general nature of the sediments in the area and the changes which take place from the coast across the shelf, slope, and trench to the ocean basin.

Mechanical Composition of Shelf Sediments

Near the coast the superficial sediment consists of sand (table 2) with a relatively small proportion of mud. This grades outwards into sand with a progressively increasing mud content, which in turn passes into mud on the outer part of the shelf. Sediment types to a few feet below the surface are similar to the superficial sediment, except at A795, where the lower part is moderately sandy mud, which is abruptly overlain by very sandy mud.*

Rock pebbles were not found in the shelf sediments (table 3), although shells or shell fragments up to several centimetres in diameter may occur in places. The sand and silt fractions in these sediments are dominantly terrigenous and contain few, if any, Foraminifera. The terrigenous material is derived almost entirely from the Mesozoic and Tertiary sedimentary rocks of the mainland, although occasional grains of rhyolitic pumice derived from Quaternary volcanic formations are also found.

*Muddy sediments containing less than 50 percent of sand are here divided into "mud", with less than 5 percent of sand; "moderately sandy mud", with 5–14 percent of sand; and "very sandy mud", with 15–49 percent of sand. In pebbly muds, the category is determined on the basis of the sand/mud ratio.

Table 2. Weight percentage of sand fractions from core samples

Sample No.	Bathymetric zone	Weight percentage of sand fractions	Main lithological components
A793/MA	Shelf	98.28	R
A795/MA1	"	27.20	R
A795/MA2	"	7.27	R
A796/MA1	"	62.45	R
A796/MA2	"	53.88	RS
A792/MA1	Slope	14.70	RS
A792/MA2	"	4.04	R
A797/MA1	Top of slope	3.25	R
A797/MA2	"	6.50	R
A798A/MA	Slope	2.20	RS
A798B/MA	"	1.98	R
A807/MA1	"	1.09	RFW
A807/MA2	"	0.51	RFW
A808/MA	"	2.89	RF
A809/MA1	"	20.58	R
A809/MA2	"	9.84	R
A809/MA3	"	0.80	RWF
E3A/MA	"	2.64	R
E3B/MA	"	2.28	R
E4A/MA	"	1.10	RF
E4B/MA1	"	1.75	R
E4B/MA2	"	0.89	RF
E4D/MA1	"	1.43	RF
E4D/MA2	"	1.63	RF
E4D/MA3	"	2.01	RF
E5/MA	"	0.70	RW
E6/MA1	"	3.87	R
E6/MA2	"	0.24	RF
E12/MA1	"	0.26	RF
E12/MA2	"	7.43	R
E13/MA1	"	0.48	RF
E13/MA2	"	0.57	RF
A791/MA	Canyon	18.80	RW
A805/MA1	"	11.81	RPF
A805/MA2	"	2.42	RF
A810/MA	"	1.66	R
E2A/MA1	"	2.67	R
E2A/MA2	"	1.17	R
E2B/MA	"	0.63	R
E10A/MA1	"	3.16	RF
E10A/MA2	"	6.36	P
E10B/MA1	"	15.60	RF
E10B/MA2	"	3.74	RFP
E11/MA	"	14.26	R
E7/MA1	Trench	0.54	RSF
E7/MA2	"	76.45	R
E8A/MA1	"	0.04	R
E8A/MA2	"	0.13	F
E8D/MA1	"	0.22	F
E8D/MA2	"	3.75	RF
E9A/MA1	Ocean basin	2.93	F
E9A/MA2	"	0.41	P
E9B/MA1	"	10.01	PF
E9B/MA2	"	3.71	P

R = Mineral grains (other than pumice fragments).
S = Shells and shell fragments (other than foraminifera).
F = Foraminifera.
P = Pumice fragments.
W = Wood fragments.
Where two or more symbols are shown, the constituents are in order of abundance.

Mechanical Composition of Slope Sediments

Across most of the continental slope the sediments consist of mud containing less than 5 percent of sand. Somewhat different sediments are found in cores A792, A797, A808, and A809, but these all occur in bathymetric environments atypical of the slope (fig. 2). A792, from much closer to Cook Strait than the other slope cores, contains pebbly mud, the pebbles being terrigenous non-volcanic rock fragments. Many of these pebbles are friable and stained brown with limonite indicating former subaerial weathering (an effect which has not been found elsewhere in the area). Core A797, at the very top of the slope, is dominantly mud but contains two layers of sand which are mechanically quite distinct from the bulk of the sediment. A808, located on a slope high west of the Pahaua Canyon (Pantin 1963, fig. 5, profiles A–A′ and E–E′), is dominantly muddy, but the upper part consists of an accumulation of mud lumps and is not a normal mud produced by the deposition of fine particles. In the uppermost part of the core, moreover, the mud lumps are partly glauconitised. A809 is situated on the same slope high, about $3\frac{1}{2}$ miles north-east of A808. The upper part of this core consists of a thin layer of very sandy mud with numerous small glauconite particles; the central part is a thicker layer of moderately sandy mud, while the lowest part is virtually sand-free mud.

In all the above sediments the sand and silt fractions are mainly terrigenous, although volcanic fragments and Foraminifera are more common than on the shelf. The origin of the different components is the same as that of equivalent material in the shelf sediments.

On the lower part of the slope, layers of laminated silt occur within the more typical

Table 3. Weight percentage of pebble fractions from core samples

Sample No.	Bathymetric zone	Weight percentage of pebble fractions	Main lithological components
A795/MA1	Shelf	0.38	S
A796/MA1	"	0.22	S
A796/MA2	"	1.31	S
A792/MA1	Slope	9.09	RS
A792/MA2	"	0.24	RS
A791/MA	Canyon	0.95	RSW
A805/MA1	"	0.12	MSP
A805/MA2	"	0.03	S
All other samples		nil	

R = Lithified rock fragments
S = Shells and shell fragments
P = Pumice fragments
W = Wood fragments
M = Mud lumps
Where two or more symbols are shown, the constituents are in order of abundance.

mud. These layers are normally 1–2 cm thick and 10–20 cm apart, are sharply defined above and below, and usually show no systematic grading. They consist predominantly of non-volcanic sandy silt, although numerous muddy laminae are generally present and coarser laminae composed of silty sand may also occur. In the lower part of a layer near the base of E12 are laminae of an unusual type, containing numerous Foraminifera. The layers of silt are visible in both cores from this part of the slope (E6 and E12), but whereas those in E6 are relatively undisturbed, many in E12 are fragmented and contorted, evidently as a result of mechanical disturbance. Highly fragmented layers may be represented by nothing but isolated pockets of laminated silt. These disturbed layers, however, are closely associated with others showing little evidence of disturbance. This type of deep-sea silt layer, containing laminated non-volcanic sediment, must be clearly distinguished from another type of silt layer which occurs at certain other localities in the area and consists of non-laminated volcanic silt.

The laminated silt layers clearly belong to the category defined as "discontinuous" by Gorsline and Emery (1959, pp. 284–5), while the intervening mud belongs to the "continuous" category (loc.cit.). However, I consider that "continuous" and "discontinuous" are ambiguous terms, since they were intended to be used in a time sense but could also be taken in a spatial sense: it might be thought that "continuous" meant a layer which persisted laterally and "discontinuous" meant a layer composed of thin disconnected lenses. For this reason, the terms "diatelic" and "adiatelic"* are proposed here to cover sediments whose deposition was respectively "continuous" and "discontinuous", all these terms being used here with a time connotation.

E6 and E12 also contain layers a few centimetres thick composed of mud with a higher proportion of silt than in the remainder of the mud in these cores. This type of sediment is herein called "silty mud". The layers of silty mud are probably adiatelic: they are usually bounded sharply above and below, and sometimes lie immediately above and in contact with the adiatelic silt layers. The silty mud, however, shows no lamination.

Mechanical Composition of Canyon Sediments

Three submarine canyons were sampled: the Wairarapa Arm of the Cook Strait Canyon; the Pahaua Canyon; and the upper part of the Madden Canyon, known as the Madden Depression (figs. 1 and 2).

Mud or moderately sandy mud predominates in all the canyon cores, but other types of sediment are also found. Pebbly mud occurs in A791 (Wairarapa Arm) and A805 (Madden Depression). Again, adiatelic layers of sand or silt occur in all three canyons. Thin layers of medium sand are found in A791, A810, and the upper part of E2a, while thicker layers of coarse sand occur in the lower part of E2a. Thin adiatelic layers of silt are present in both E10a and E10b (Madden a significantly higher proportion of sand than the rest of the sediment, although still predominantly significant proportion of rhyolitic pumiceous silt or sporadic sand-size rhyolitic pumice grains.

Layers up to about 10 cm thick which contain a significantly higher proportion of sand than the rest of the sediment, although still predominantly muddy, are common in E10a and E10b. Similar layers occur in the Pahaua Canyon cores and in core E7 from the Hikurangi Trench. These layers contain numerous small muddy aggregates (1–3 mm in diameter) and are here called "sandy layers with aggregates". These aggregates, which are evidently faecal pellets, are distributed in irregular, poorly defined concentrations, and thus give rise to mottling.

Most of the sandy layers with aggregates show strong evidence of disturbance by burrowing organisms. Bulges at the upper and lower contacts may represent impressions left by parts of animals. However, internal lamination occurs in some of the layers near the base of E10b; these layers consist of moderately sandy mud and faecal pellets in various proportions, with occasional very thin laminae of sand.

A few of the sandy layers with aggregates in E10a contain small irregular pockets of several quite distinct types of sediment and these are probably layers in which an original well developed lamination has been almost obliterated by organic burrowing.

At the very base of E10a, in the Madden Depression, there is a layer of non-laminated silt consisting almost entirely of rhyolitic glass fragments. This volcanic silt is very distinctive and the layer is quite clearly different in origin from the laminated non-volcanic silt layers observed on the lower part of the slope.

Colour of Mud Component in Shelf, Slope, and Canyon Sediments†

The mud component in these sediments varies in colour from pale olive, through pale sub-olive (with a faint olive chroma), to pale grey with no significant olive chroma. There are apparently two main varieties which will be called "olive mud" and "grey mud" according to whether a significant olive chroma is present or not. This colour difference is well developed in the clay fractions but only poorly developed in the silt fractions and appears to be absent from the sand fractions associated with the two types of mud. Evidently,

*These terms are derived from the Greek *diatelos* meaning continuous.

†Colour descriptions refer to dry sediment, unless otherwise stated. Wetting the sediments causes them to become somewhat darker, but does not alter the hue.

the bulk difference in colour is due to some physical or chemical difference in the clay fractions. Various tests were made in connection with the present work to determine the clay mineralogy of the olive and grey muds and the reason for their colour difference (see p. 35). It appears that the olive hue is caused by degradation products of chlorophyll known collectively as "pheophytin", the latter being adsorbed on to mineral particles (principally the clay fraction).

Many shelf and slope cores contain only olive mud from top to bottom. In contrast, in two cores from the Pahaua Canyon (E2b and E11) the mud is almost all grey. A third group of cores contains olive mud in the upper part and grey (or pale sub-olive) mud in the lower part; in these the downward transition may be abrupt (as in A795), gradational (as in E13), or interbanded (as in A797, A807, A809, and A810). Only two cores, both taken on the slope (E4d and E5), show the olive chroma increasing downwards and in both the olive chroma in the lower part of the core is poorly developed.

Under natural conditions the grey mud is normally more compact than the olive, this being clearly shown by the slope and canyon cores in which grey mud extends to the top of the core (E2b, E4d, E5, and E11). Core E4d however, is atypical: it consists of mud that was hard even when collected, being far more compact than the mud in any of the other cores. The shape of this core is also abnormal: it comprises three portions, each of which narrows gradually towards the top, this narrowing being compensated by an abrupt increase in diameter at the base of the two upper sections. This shape indicates that either the corer struck the sea bed at least three times, giving three very short superimposed cores, or that the corer penetrated three naturally superimposed slabs of hard mud.

Colour and Provenance of Sand Component in Shelf, Slope, and Canyon Sediments and Comparison with Silt Component

The terrigenous non-volcanic sand and silt components in these sediments are mainly of quartz and greywacke fragments together with some feldspar and argillite. The colour of the non-volcanic sand component ranges from medium to pale grey, sometimes with a faint olive or purple hue. Variations in colour are due to variations in the ratio of quartz and feldspar to greywacke and argillite fragments. The non-volcanic silt component ranges from grey to very pale grey, with or without a faint olive or purple hue: these variations in the silt must be due, at least in part, to variations in the relative proportions of clastic minerals, but the colour of the silt will also be affected to some extent by the factors that control the difference between the olive and grey muds. These factors, which apparently do not include variations in clastic mineral content, are discussed on p. 36.

The rhyolitic pumice, presumably derived from the similar Quaternary volcanic deposits of the Taupo region, is very light in colour (white to very pale grey). This is most conspicuous in the rhyolitic silt layer at the base of E10a, which is almost pure white and contains virtually no mud.

Foraminifera, when they occur, are light-coloured but are rarely sufficiently numerous to have much effect on the colour of the sand or silt components.

Mechanical Composition and Colour of Hikurangi Trench Sediments

Cores were taken from two places near the axis of the Hikurangi Trench: E7 was taken near the south-western end of the trench, opposite Cook Strait, while E8a and E8d were taken about 60 miles to the north-east. The latter consist dominantly of pale olive, very pale olive, or pale sub-olive slightly foraminiferal hemipelagic mud, containing only a small proportion of terrigenous sand. This mud is interspersed with adiatelic silt layers, which are mainly laminated sandy silt, although muddy laminae are present in some cases. The silt is grey to pale grey: terrigenous grains are always dominant and are usually the only significant component. The adiatelic layers average 1–12 cm in thickness, and are 5–50 cm apart; they usually show no systematic grading. In both E8a and E8d some of the silt layers are broken up or distorted as a result of mechanical disruption involving the adjacent muddy sediment but other layers immediately above and below may show no significant disturbance.

E7 is altogether different from E8a and E8d. The upper 14 cm consists of pale olive hemipelagic mud, which is underlain by a sandy layer with aggregates 10 cm thick consisting of pale olive moderately sandy mud in which the mud is mainly concentrated in aggregates 1–3 mm in diameter and the sand mainly in very small irregular pockets up to 1 mm in diameter. This layer is underlain by an adiatelic layer of about 175 cm of muddy sand, light to medium grey, and varying from medium-fine to medium-coarse in texture. The sand contains a high proportion of mica and plant fragments compared with the sand fraction of any of the other cores. The thickness of the sand layer may well be considerably more than 175 cm, for the corer may not have reached the base of the layer. No bedding can be seen, but paramictic structure occurs in several places.

Mechanical Composition and Colour of Ocean Basin Sediments

The two cores taken in the ocean basin (E9a and E9b) are very similar to one another. They consist dominantly of pale to very pale sub-olive foraminiferal pelagic mud, though E9b contains occasional zones of similar but moderately sandy

mud. The sand fraction contains very little terrigenous material and is dominantly of Foraminifera and white rhyolitic pumice in various proportions.

Near the base of both cores is a layer of white non-laminated silt several centimetres thick, composed almost entirely of rhyolitic pumice fragments with a small admixture of mud.

Mechanical Composition of Mud Fractions

The mechanical composition of the mud fraction (less than 63 microns) was determined by the pipette method for a series of samples covering all of the main bathymetric zones. The results (table 4) show that the shelf sediments possess a consistently higher ratio of coarse + medium silt to fine silt + clay than sediments in the other bathymetric zones. However, the number of measurements is too limited, and the range of observed values is too great, to determine whether or not this ratio varies significantly between slope, canyon, trench, and ocean basin.

Table 4. Weight ratios of coarse + medium silt (63 to 8 microns) to fine silt + clay (< 8 microns)

Sample No.	*Bathymetric zone*	*Ratio*
A795/MA1	Shelf	58:42
A795/MA2	"	49:51
A796/MA1	"	55:45
A796/MA2	"	51:49
A807/MA1	Slope	44:56
A807/MA2	"	29:71
E4A/MA	"	41:59
E4B/MA2	"	41:59
E5/MA	"	29:71
E6/MA2	"	31:69
E12/MA1	"	29:71
E2A/MA2	Canyon	39:61
E2B/MA	"	38:62
E8A/MA2	Trench	25:75
E8D/MA1	"	28:72
E9A/MA1	Ocean Basin	28:72
E9B/MA1	"	41:59

Mineralogy of the Clay-size Fractions

X-ray diffractometer measurements on a series of samples (table 5) show that chlorite and a micaceous mineral (presumably illite) are the dominant crystalline clay minerals throughout the area. Infrared absorption spectrograms further show that calcite and quartz are present in all samples, and that allophane occurs in all but one (E13/X2). The highest values for calcite are found in the core from the ocean basin (E9a), while the values in the core from the trench (E8a) are intermediate between those of the ocean basin and those of cores taken nearer to the coast.

Table 5. Analysis for clay-size minerals by infrared absorption spectrometer

Absolute values for calcite could not be determined by the method and the figures are expressed as a percentage of the maximum value determined (sample E9A/X1).
(N.B. X-ray diffraction showed chlorite and mica (illite) to be the dominant crystalline clay minerals.)

Sample	*Lithology*	*Bathymetric zone*	*Allophane*	*Mica (illite)*	*Quartz*	*Calcite*
			Approx. weight percent of total allophane + mica + quartz			
A795/MA1	Pale olive very sandy mud	Shelf	7	39	54	17
A795/MA2	Pale grey moderately sandy mud	Shelf	5	44	51	11
A807/MA1	Pale olive mud	Slope	9	34	57	27
A807/MA2	Pale sub-olive mud	Slope	8	45	47	15
E13/X1	Pale olive mud	Slope	13	45	42	30
E13/X2	Pale grey mud	Slope	—	54	46	21
E2A/X1	Pale olive mud	Canyon	13	47	40	26
E2A/X2	Pale olive mud	Canyon	13	33	54	29
E2B/X1	Pale grey mud	Canyon	6	44	50	20
E2B/X2	Pale grey mud	Canyon	13	27	60	20
E8A/X1	Very pale olive mud (pale alteration burrow)	Trench	11	46	43	64
E8A/X2	Pale olive mud (matrix around pale alteration burrow)	Trench	12	50	38	48
E9A/X1	Very pale sub-olive mud (pale alteration burrow)	Ocean basin	7	36	57	100
E9A/X2	Pale sub-olive mud (matrix around pale alteration burrow)	Ocean basin	7	39	54	90

The current at any point in the sea may be regarded as the vector sum of a series of components resulting from a series of different physical effects. While all these effects will in fact be superimposed, their relative importance will vary considerably from one place to another. It is therefore convenient to enumerate these components separately to evaluate their probable magnitude in different parts of the sea.

1. Wave Turbulence

In this category may be included all the eddies and rip currents associated with normal (wind-driven) waves as well as the swash and backwash of breaking waves. This type of turbulence dies away rapidly with depth but is powerful in shallow water; it stirs a great deal of fine-grained sediment into suspension on the shallow parts of the continental shelf, and moves a significant amount of coarse sediment by traction.

Concentration of sediment suspended by wave action decreases away from the shore because of the greater depth, and this causes seaward transport of sediment as a result of the eddy diffusion effect. If the concentration of suspended sediment in the sea varies from one place to another, eddy diffusion (if present) will result in a net transport of sediment down the concentration gradient. The rate of transport will be proportional to the concentration gradient and to the eddy diffusion coefficient. Wave turbulence will be effective in transporting sediment mainly on the shallower parts of the shelf where concentration gradients of sediment are highest and where eddy diffusion resulting from waves is also at a maximum. Theoretically, any grain size can be transported, but the process will be most effective for mud and sand, which are carried much more easily than coarser material.

Since the bottom current velocities associated with wave turbulence decrease away from the shore, the transporting power of these currents must also decrease. The average grain size of the sediment transported and deposited by wave turbulence will therefore decrease progressively seawards. A possible result of this effect would be the deposition of a belt of sand near the coast, grading outwards through muddy sand into sandy mud.

This particular distribution of sand and mud was at one time accepted as the "normal" situation on continental shelves, probably as a result of a tacit (but incorrect) assumption that wave turbulence is always the dominant factor in shelf sedimentation. It has become clear (Shepard 1963, pp. 258–9) that a sand belt followed seawards by a mud belt is by no means the "normal" situation on the shelf. This distribution may, however, be found in shelf areas where sedimentation is in fact controlled mainly by wave action.

2. Turbidity Effect

Any body of sea water containing suspended sediment will have a greater effective density than adjacent clear sea water if temperature and salinity are roughly similar. The effective density of the turbid water will cause it to sink below the clear water and flow along the sea bed in a downward direction. The rate of flow depends on the density of the suspension, the thickness of the turbid water mass, and the prevailing gradient of the sea bed. This type of flow is here called the "turbidity effect" and must occur virtually all the time along every coast wherever sediment is stirred into suspension by wave turbulence. In fact, "wave action", meaning the overall seaward transport of sediment by waves, must include the superimposed results of the eddy diffusion effect and the turbidity effect.

A "turbidity current" may be defined as any current in which the predominant velocity component is due to the turbidity effect. The turbidity effect will in fact operate whenever sediment is stirred into suspension by bottom currents, whatever their origin, or by submarine slumping. The magnitude of the effect, however, will be significant only when the concentration of suspended sediment is high or the submarine gradient is steep. The effect will thus be most pronounced on the continental slope, particularly in submarine canyons, but may also be significant on parts of the shelf where a high concentration of suspended matter might compensate in part for the usually gentle gradients.

Two fundamental types of turbidity flow are theoretically possible. Any current involving turbid water will have two components: the turbidity component and that due to currents of other types. If the velocity of the turbidity component is not sufficient in itself to keep the contained sediment in suspension, the flow will not persist if the non-turbidity component is removed. The sediment will gradually settle out and the flow will slow down, eventually coming to rest. This kind of turbid flow cannot persist over a long period unless energy is supplied from outside, for instance by slumping or wave stirring, and is therefore called here "allodynamic turbidity flow" (ATF).

If, however, the turbidity component of the bottom current is sufficient (or more than sufficient) to keep the sediment in suspension, the flow will persist by virtue of its own gravitational energy even if the non-turbidity component of the current ceases entirely. This is the state known as "auto-suspension" (Bagnold 1956, p. 270, and 1963, p. 518; Middleton 1966, p. 206). A turbidity flow of this type tends to pick up sediment from the sea bed, if it is of easily erodable material. The acquisition of extra sediment will make the flow travel faster, and this in turn will

increase its sediment-carrying capacity. The result is a self-propagating reaction with the velocity of the flow and the sediment content increasing simultaneously. The process will be halted only if the submarine gradient decreases, if the supply of erodable material on the sea bed runs out, or if the flow becomes so turbid that its capacity to pick up further sediment is seriously impaired. This type of flow, depending only on its own gravitational energy, is here called "ideodynamic turbidity flow" (ITF). For any given turbid current, ATF will pass into ITF once the turbidity component of the velocity has reached a certain value. This velocity, which will be constant if the gradient, flow thickness, and sediment type are specified, will be called the "auto-suspension velocity" (ASV).

Although ATF must be very widespread and virtually continuous, its intensity will fluctuate in space and time through local variations in bottom currents or periodic slumping. ATF will pass into ITF under suitable conditions, which will be localised in both space and time. Steep gradients and a heavy sediment content are essential for ITF; it is therefore probable that the initiation of ITF will be confined to submarine canyons and other features with steep negative relief and will only occur when there is a sudden influx of suspended sediment, for instance during a heavy storm, after an exceptionally large slump, or during a heavy flood at the mouth of a major river. It should be noted that these conditions will in any case give rise to the most intense phases of ATF whether ITF occurs or not.

ITF is probably very rare on the shelf owing to the prevailing low gradients. On the other hand, when ITF occurs on the slope, or more particularly in canyons, the currents might well continue along a trench or across the floor of an ocean basin. This could happen if the density of the flow were sufficient to perpetuate ITF across the relatively low gradients of the deep sea floor, or if the momentum of the flow were sufficient to carry it forward even if the velocity fell below the ASV.

Numerous authors have used the terms "turbidity currents" or "a turbidity current" to explain various sedimentary phenomena, in particular deep-sea sand layers and sandstone units in flysch-type beds, which have come to be known collectively as "turbidites." However, these authors do not usually distinguish the two fundamental types of turbidity flow. "Turbidity currents", as used in the literature, are assumed to be temporary and relatively local phenomena, but it is rarely made clear whether they are considered to be phases of ITF or merely statistical peaks in the general ATF background.

In spite of these uncertainties it seems reasonable to suppose that the highly distinctive "turbidite" beds, which are evidently deposited by some kind of discontinuous process, correspond to phases of ITF.

3. Tidal Currents

All seas and oceans are affected by tidal currents. These are relatively weak over most of the ocean but locally become very powerful wherever they are constricted either horizontally or vertically. Horizontal constriction occurs in narrow channels particularly when the channel is the only breach in a long ridge of land: Cook Strait is a good example of this effect. Vertical constriction occurs over the edges of continental shelves and over the tops of shallow banks.

Since tides are cyclic phenomena, it might be expected that the tidal component of bottom currents would have little overall effect on sediment transport through opposite phases of the cycle cancelling out. However, the tide may have a residual vector superimposed on the cyclic component, leading to a net transport of sediment in the appropriate direction. Again, tidal currents may have a considerable effect by stirring sediment into suspension and increasing the amount of turbulence. This would amplify both the eddy diffusion effect and the turbidity effect. In many areas the main effect of tidal currents is to remove fine sediment fractions from the areas where currents are strongest leaving a layer of relatively coarse relict sediment.

4. River Outflow Effect

When a river reaches the sea the outflowing water fans out and rapidly loses velocity. Nevertheless, a relatively gentle seaward flow continues beyond the river mouth taking with it any sediment suspended in the river water.

Normally this outflow takes place on the surface (hypopycnal flow: Bates 1953, p. 2125), but occasionally the sediment content of the river water is sufficient to raise its effective density above that of sea water, in which case the river water flows along the bottom (hyperpycnal flow: Bates 1953, p. 2125). Sediment settles out progressively during hypopycnal flow, and in most cases this is also true of hyperpycnal flow. The latter generally takes the form of ATF, but in a few extreme cases ITF may be set up.

When rivers are small the outflow is broken up by waves and general turbulence, and the sediment-transporting capacity is reduced to negligible proportions except possibly during floods. In large rivers, however, the magnitude of the outflow is sufficient to swamp the effects of marine turbulence and significant quantities of sediment may be carried seawards for considerable distances. In hypopycnal flow and hyperpycnal ATF, sediment will usually be deposited locally in the form of a rain of relatively fine particles. On the other hand, if hyperpycnal ITF were initiated, large quantities of relatively coarse material would probably be transported and deposited a considerable distance from the river mouth.

5. Ocean Currents

Although all the types of current mentioned operate in the ocean, and are therefore in one sense "oceanic", the term "ocean currents" is normally confined to large-scale oceanic water movements persisting over long periods. This broad definition includes currents such as the Gulf Stream, the Kuroshio, and the Humboldt Current. These currents are normally slow except in localised streams or constricted channels. They include two main types, which may be superimposed to a greater or lesser extent: gradient currents, caused by variations in water density due to changes in temperature and salinity; and drift currents due to prevailing winds, caused by persistent wind shear at the sea surface.

Ocean currents appear to be too weak in most areas to do more than transport material already in suspension, but when constricted horizontally or vertically, or when flowing in a localised stream, they may become sufficiently powerful to stir up sediment on the sea bed, and in these areas there is formed a layer of relatively coarse relict sediment, the finer material having been removed in suspension. Unlike tidal currents, ocean currents have a dominant vector component, and sediment can be directly transported from one locality to another by this vector component as well as indirectly by amplification of the eddy diffusion effect and the turbidity effect. Near land, however, the vector components of ocean currents show a strong tendency to run parallel to the coastline, and significant removal of sediment from the shelf and slope will occur only where the currents run obliquely away from the coast.

6. Storm-drift Currents

These are produced in the same way as drift currents due to prevailing winds, but are stronger and more localised. The movement is mainly confined to the uppermost layer of water, which implies that the effect of storm-drift currents will be significant only on the shelf. In this bathymetric zone large quantities of sediment could be transported by such currents, which, in addition, would amplify the eddy diffusion and turbidity effects. The result of a storm drift would probably be to stir up sediment for a short period removing the finer fractions and leaving a layer of relatively coarse sediment. This would eventually be covered by the more typical sediments of the area which would have smaller average grain size. Since storm drift would last only a few days, in most cases the coarse layer resulting from a wind-drift episode would probably be thinner than the coarse relict layers produced by the long-lasting tidal and ocean currents.

Near the coast the constraining effect of the land would cause direct transport by storm drift to be orientated mainly parallel to the coast, but further out a significant component can develop obliquely to the coast. This is particularly true of onshore winds with a long fetch which may drive water shorewards in the form of a wind surge.

7. Giant Eddies

When wind-drift currents impinge on the coast the flow component normal to the coastline causes the water to pile up, and the sea surface rises. On a wide, shallow shelf this increase in hydrostatic head cannot readily be compensated by a deeper current with an off-shore component. If, however, wind-drift currents impinge on a narrow shelf bordered by considerably deeper water, the build-up of water pressure is partly counteracted by a flow of deeper water with a component away from the shore. Similarly, an offshore wind may lower the sea surface to a certain extent, causing the upwelling of deeper water. However, the magnitude of this effect is relatively small compared with the strength of currents produced by onshore winds. These currents and counter-currents are sometimes associated with large-scale turbulence, or "giant eddies". Some of these eddies are believed to extend across the base of the slope on to the ocean floor, while others become locally powerful in submarine canyons. It is probable that in some localities these currents are strong enough to transport considerable quantities of mud and sand. As in storm drift, the effect of giant eddies would probably be to stir up sediment for a limited period, removing the finer fractions and leaving behind the coarser material. The occurrence of giant eddies might thus be shown by local relatively coarse layers within the prevailing fine-grained sediment on the slope or the ocean floor.

8. Tsunami-generated Currents

Tsunami, when they travel across the ocean, consist of very long waves moving at 400–500 knots with periods ranging from 10 minutes to 1 hour, although 15–20 minutes is usual. The total range of wavelength is thus about 80–500 miles, but the majority have a wavelength between 120 and 170 miles.

These wavelengths are much greater than the depth of the water, and for this reason the pressure variations associated with the passage of a tsunami extends to the sea bed. This gives rise to oscillating bottom currents, but it can be shown that these are very weak in the open ocean. The approximate average velocity of the currents may be calculated using the formula:

$$V_c = \frac{2aV_t}{\pi h} \qquad (1)$$

where V_c = average scalar velocity of the bottom currents, a = surface amplitude of the tsunami, V_t = tsunami wave velocity, and h = depth of water.

This formula gives a bottom current velocity of only about 0.1 knots for a tsunami with amplitude 6 ft, period 20 minutes, and wavelength 140 miles, in water 16,000 ft deep. Velocities of this order would certainly be capable of transporting a thin carpet of relatively fine sediment across the sea bed, but since the currents are oscillating the movements back and forth will virtually be cancelled out and there is not likely to be any significant removal of sediment from a particular area. Any sediment stirred into suspension by these weak currents would settle out close to its original position, but such an event could possibly be identified by the presence of a thin graded layer consisting of the same type of material as the associated pelagic sediment.

Much stronger currents occur when tsunami approach shallow water. The standard formula for the velocity of propagation of a tsunami is:

$$V_t = \sqrt{gh} \qquad (2)$$

where h is the depth of water. Combining equations (1) and (2) gives:

$$V_c = \frac{2a}{\pi h}\sqrt{gh}$$

$$= \frac{2a}{\pi}\sqrt{g/h} \qquad (3)$$

Even if the amplitude remained constant, (3) shows that V_c must increase as h decreases. In fact, when a tsunami approaches the continental shelf the amplitude increases considerably and the wave velocity V_t falls at the same time.

Assuming an amplitude of 6 ft, and a depth of 400 ft near the edge of the shelf, (3) gives a current velocity of $\frac{2}{3}$ knot. Still higher values might occur on the central shelf, but velocities would again decrease near the coast because of bottom friction and the constraining effect of the land. Currents of $\frac{1}{2}$–1 knot would be capable of stirring up considerable quantities of medium- to fine-grained sediment on the outer part of the shelf; conditions near the shelf-edge would also be favourable for the removal of the suspended sediment by the turbidity effect, by tidal currents, and by ocean currents. Tsunami currents near the shelf-edge would thus be likely to give rise to a layer of relatively coarse relict sediment. Separate tsunami would be recorded by a series of coarse relict layers intercalated in finer-grained sediments.

Classification of Sediment-transporting Mechanisms

It is convenient to classify the various sediment-transporting mechanisms in terms of two parameters: (i) the relative amounts of sediment transported when the mechanisms are operating at normal intensity and (ii) the variation of the intensity with time. Each mechanism may be classified qualitatively as first, second, third, or fourth order depending on its sediment-transporting capacity, this decreasing from first to fourth order. These categories may be divided in turn into continuous, cyclic, variable, and discontinuous, according to whether or not the intensity of the mechanism varies with time (table 6).

Table 6. Probable relative importance of sediment transporting mechanisms and changes in relative intensity with environment.

Mechanism	*Shelf*	*Open slope*	*Slope highs*	*Canyons*	*Trench*	*Ocean basin*
Wave turbulence	1V —2V	3V	3V	4V	4V	4V
ATF	3V	3V	4V	2V	4V	4V
ITF	1D (very rare)	1D (very rare)	(probably unknown)	1D	1D	1D (rare)
Peripheral currents around zones of ITF	2D —3D	2D	4D	2D	2D —3D	3D —4D
Tidal currents	1Y —4Y	3Y —4Y	2Y	4Y	4Y	4Y
River outflow	2V —4V	3V —4V	3V —4V	3V —4V	4V	4V
Ocean currents	4C	3C	2C	4C	4C	3C
Storm drift	1D —3D	2D —4D	2D —4D	4D	4D	4D
Giant eddies	4D	3D	3D —4D	2D —3D	3D	4D
Tsunami currents	1D —3D	2D —4D	3D —4D	4D	4D	4D

1 = First order (greatest intensity)
2 = Second order
3 = Third order
4 = Fourth order

C = Continuous
Y = Cyclic
V = Variable
D = Discontinuous

NATURE AND ORIGIN OF INTERNAL STRUCTURES

The internal structures in the sediments of the area may be divided into two main categories: inorganic and organic. Both include numerous subdivisions which will be described, together with their probable modes of origin, in the following sections.

CLASSIFICATION OF INORGANIC STRUCTURES

The inorganic structures may be classified as follows:

- Bedding
  - Banding (units > 1 cm thick)
  - Lamination (units < 1 cm thick)
- Transition planes
- Convective paramictic structures
- Slump structures
  - Paraautochthonous
    - Structures associated with paramictic slumping
    - Structures associated with shear-plane slumping
  - Allochthonous
    - Structures associated with creep-slumping
    - Structures associated with mudflows and sandflows

The term "banding" is conventionally used for stratifications where units are more than 1 cm thick, while "lamination" is used where the units are less than 1 cm thick. For sediments containing turbidites and other adiatelic beds the distinction between bands and laminae is often difficult to apply, since thin adiatelic "laminae" sometimes alternate with considerably thicker "bands" of diatelic sediment. Accordingly, it is convenient to distinguish banding and lamination in sediments with adiatelic layers by referring only to the thickness of the adiatelic layers themselves.

Banding and Lamination

Numerous examples of banding and lamination are shown in the core stratigraphy diagrams (figs 3–8). Banding is illustrated in figs 9–12 while lamination is illustrated in figs 9, 10, 12, 13, and 14.

Banding is rare in the shelf sediments. When it occurs it takes the form of poorly defined units a few centimetres thick, the units being distinguished by slight to moderate differences in sand:mud ratio. The boundaries of units are usually diffuse and are often profoundly disturbed by burrowing organisms.

Faint coarse lamination is occasionally seen in the shelf sediments, but as in the larger-scale bedding, the boundaries are diffuse and often highly disturbed by burrowing organisms. In these sediments, moreover, true lamination is difficult to distinguish from the relatively more abundant pseudolamination, which is organic in origin.

The banding and lamination in the shelf sediments could, in theory, be produced either by variations in current strength or by variations in sediment supply. An increase in current strength on the shelf would almost certainly give rise to an increase in the maximum size of particles in the sediment, since coarser material is readily available. However, the observed maximum grain size of the sand fraction is roughly similar in adjacent bands whatever the difference in sand:mud ratio, and it is thus probable that there has not been much variation in current strength between the deposition of one band and the next. If so, the banding must be due mainly to variations in sediment supply. These variations could be (a) changes in the sediment supplied by wave action resulting from slight changes in sea level or (b) changes in the sediment supplied by rivers and streams resulting from changes in rainfall or vegetation cover.

Three types of stratification occur on the upper slope. The first type, which is moderately common, takes the form of faint lamination; this is made up of units which normally have diffuse boundaries and which are, in most cases, only slightly differentiated from one another. This type of stratification, which is due principally to variations in the content of small plant fragments, shows a distinct tendency to become more conspicuous in the lower parts of cores, 50–100 cm below the surface. The second type of stratification, less common than the previous type, takes the form of moderately conspicuous lamination; this is caused by the presence of diffuse layers with a slightly higher proportion of sand than in the bulk of the sediment. The maximum grain size in these sandy layers does not appear to be significantly greater than in the rest of the sediment. This type of lamination is not sufficiently common to determine whether its abundance varies with distance below the surface.

LEGEND FOR FIGS 3–8

ADL = adiatelic layer
MA = mechanically analysed samples
X = other samples
Ph = core section photographed and illustrated.

Colour terminology used for chroma: olive = definite olive chroma. (The hue is approximately 10Y, but the chroma (saturation) does not usually exceed 1 on the scale of the Rock Colour Chart (Geological Society of America, 1963; Pantin, 1969)); sub-olive = poorly developed olive chroma; grey = no significant chroma. The darkest sediments have no qualifying terms; but increasing lightness is indicated by the words pale or very pale.

Terms indicating the relative proportions of sand and mud are: mud—mud with an inconspicuous sand fraction (< *ca.* 5%); moderately sandy mud—mud with a moderately conspicuous sand fraction (*ca.* 5–14%); very sandy mud—mud with a conspicuous sand fraction (15–49%); very muddy sand—sand containing 30–50% of mud; and muddy sand—sand containing 10–29% of mud.

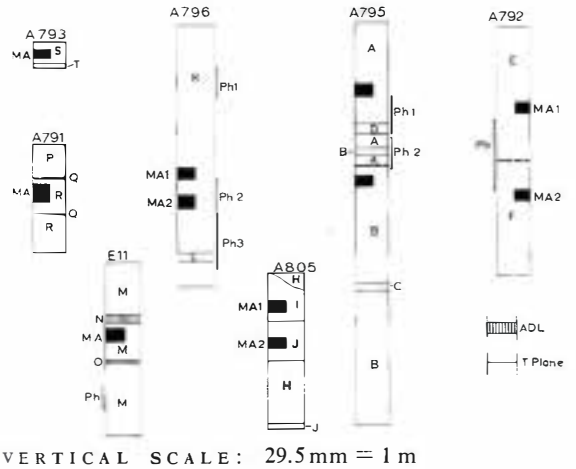

VERTICAL SCALE: 29.5 mm = 1 m

FIG. 3. Stratigraphy of cores A791, A792, A793, A795, A796, A805, and E11.

A791: Pale olive very sandy mud with (P) conspicuous lamination and (R) greywacke pebbles and faint lamination, containing (Q) distorted thin muddy sand layers.

A792: (E) pale olive pebbly very sandy mud, pebbles and shell fragments up to 1.5 cm; overlying (F) grey mud with faint general lamination and occasional friable weathered pebbles and rare shell fragments. The pebbles in (F) range up to 1 cm and the shell up to 2 cm.

A793: (S) medium grey sand; overlying (T) similar layer but with numerous shells and shell fragments up to 1 cm in diameter.

A795: (A) pale olive very sandy mud; overlying (B) pale grey moderately sandy mud with occasional shell fragments. (C) a layer of pale grey very sandy mud and (D) a bed with lithology as (A) but with small shell fragments. Upper mechanically analysed section (black) is MA1, lower is MA2.

A796: (K) pale olive very muddy sand with moderately common shell fragments; (L) a bed of similar lithology but with large shell fragments. Lowest horizon is K.

A805: (H) pale olive mud interbedded with (J) pale olive mud containing more sand than (H), and (I) pebbly moderately sandy mud with fragments of rhyolitic pumice and soft mudstone.

E11: (M) pale grey moderately sandy to very sandy mud with pumice and muddy aggregates; two adiatelic layers are present, (N) very muddy sand with relatively few aggregates, and (O) very sandy mud containing more sand than (M).

Muddy and silty sediments are termed mud, silty mud, muddy silt, and silt; these are distinguished on the basis of their physical characteristics in hand specimen. As the silt:clay ratio increases, the degree of cohesion changes from high to low, and the texture from amorphous to microgranular, while the range of chroma diminishes from olive-grey, through sub-olive-grey, to grey.

The *vertical scale* of the core diagrams is given with each figure; the *horizontal scale* is arbitrary.

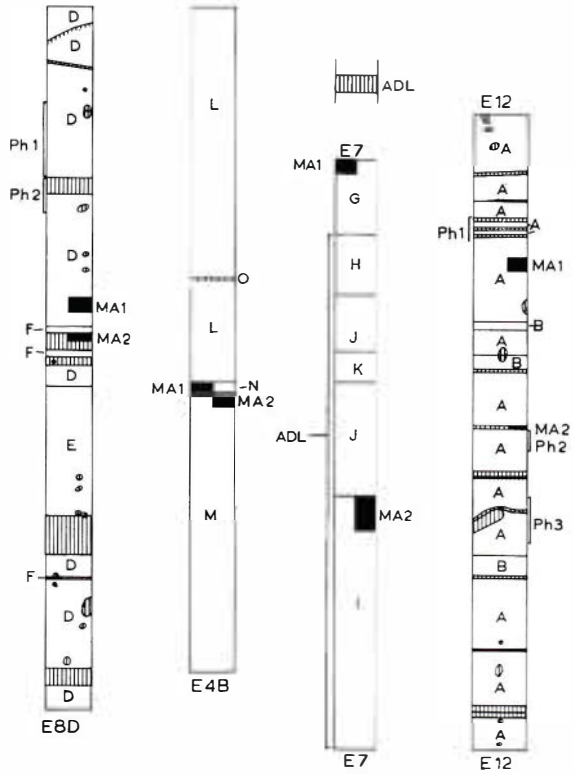

VERTICAL SCALE
E8D, E4B, E7: 38.7 mm = 1 m
E12: 27.6 mm = 1 m

FIG. 4. Stratigraphy of cores E4B, E7, E8D, and E12.

E4B: (L) pale olive mud; (M) the same with lamination; (N) the same with thin silty layers; (O) fragmented sandy layer.

E7: (G) relatively thin layer of pale olive hemipelagic mud (15 cm), overlying a more sandy layer with abundant muddy aggregates (10 cm); this is underlain by a thick adiatelic layer consisting of (H) muddy medium-fine sand, (I) muddy medium sand, (J) muddy medium-coarse sand, and (K) muddy medium sand with plant fragments. Paramictic structures are occasionally conspicuous.

E8D: (D) mud with forams, pale to very pale olive or pale sub-olive with adiatelic layers of laminated silt or muddy silt (evidently turbidites), and pockets of silt representing the disrupted remains of such layers; the silt is grey to pale grey, but acquires an olive chroma as the clay content rises. There also occurs a layer (E) consisting of very silty mud with paramictic structures, and a few thin layers (F) similar to (D) but with lamination.

E12: (A) pale olive mud with adiatelic layers of laminated silt or muddy silt (turbidites) and pockets of silt (disrupted turbidites); the silt is grey to pale grey, but acquires an olive chroma as the clay content rises. (A) also contains a few layers of sub-olive silty mud; layers of moderately sandy mud (B) are also present.

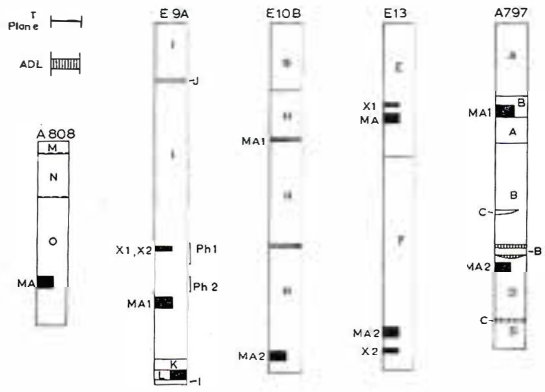

VERTICAL SCALE: 27.5 mm = 1 m

FIG. 5. Stratigraphy of cores A797, A808, E9A, E10B, and E13.

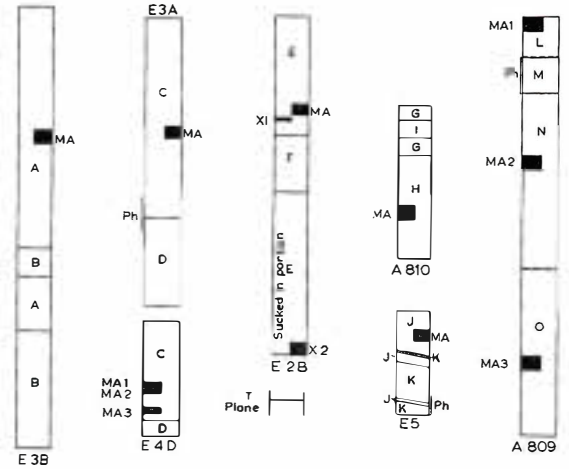

VERTICAL SCALE: 30.8 mm = 1 m

FIG. 6. Stratigraphy of cores A809, A810, E2B, E3A, E3B, E4D, and E5.

A797: Mud or moderately sandy mud, (A) pale olive, (B) pale grey; (D) similar to (B) but with faint general lamination. There also occur (i) two adiatelic layers of medium-grey sand, and (ii) two layers within the mud showing more distinct lamination (C).

A808: (M) olive to pale grey mud with glauconitic and limonitic mud lumps overlying (N) pale grey mud containing mud lumps without glauconite or limonite and (O) pale grey mud without mud lumps.

E9A: (I) pale to very pale sub-olive mud with numerous forams; (J) the same, but moderately sandy. Near the base there occurs a layer (K) of white silt consisting almost entirely of pumice; this is immediately underlain by (L), another pumiceous silt layer slightly coarser than (K). Xl is a pale alteration burrow; X2 is the matrix of the burrow. Lower black section is MA2.

E10B: (G) zone of pale olive mud grading rapidly down into (H) very pale olive mud. Numerous thin relatively sandy layers throughout, many with muddy aggregates. Occasional thin adiatelic layers of muddy silt.

E13: (E) pale olive mud with no lamination grading down into (F) pale grey mud with conspicuous lamination. Upper MA should be MA1.

A809: (L) pale olive very sandy mud with abundant glauconite at the top; (M) pale grey moderately sandy mud; (N) pale sub-olive moderately sandy mud; (O) virtually sand-free grey mud. (M) and (N) contain numerous mud pellets, some slightly glauconitic.

A810: (G) pale olive mud or moderately sandy mud varying to (H) the same but pale grey; both with well developed lamination. Just below the top are (I) interbedded pale olive and pale grey layers.

E2B: (E) pale grey mud; (F) the same with faint lamination. Occasional thin relatively sandy layers with aggregates.

E3A: (A) pale olive mud; (B) the same with faint lamination.

E3B: (A) pale olive mud; (B) the same with faint lamination.

E4D: (C) hard pale grey mud overlying hard pale olive mud and silt (D).

E5: (J) pale to very pale grey and (K) pale olive to pale sub-olive mud with faint horizontal lamination and diagonal shear-planes.

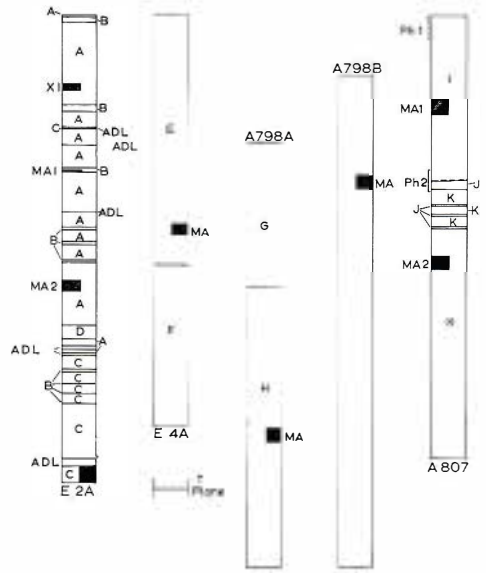

VERTICAL SCALE
E2A, E4A, A798A, A807: 29.7 mm = 1 m
E798B: 24.8 mm = 1 m

FIG. 7. Stratigraphy of cores A798A, A798B, A807, E2A, and E4A.

A798A: (G) pale olive moderately sandy mud overlying (H) pale olive mud with faint general lamination.

A798B: pale olive mud.

A807: (I) pale olive mud overlying (J) pale grey mud and (K) pale sub-olive mud. (*Note:* Ph2 bar should extend slightly higher.)

E2A: (A) pale olive mud; (C) the same with faint lamination. These are interbedded with (i) numerous thin relatively sandy layers (B) with muddy aggregates, and (ii) a few adiatelic layers (ADL) of coarse sand. (*For* D, *about one-third up, read* ADL.)

(*Note:* X2 was taken from lowest C layer.)

E4A: (E) pale olive mud; (F) the same with faint lamination.

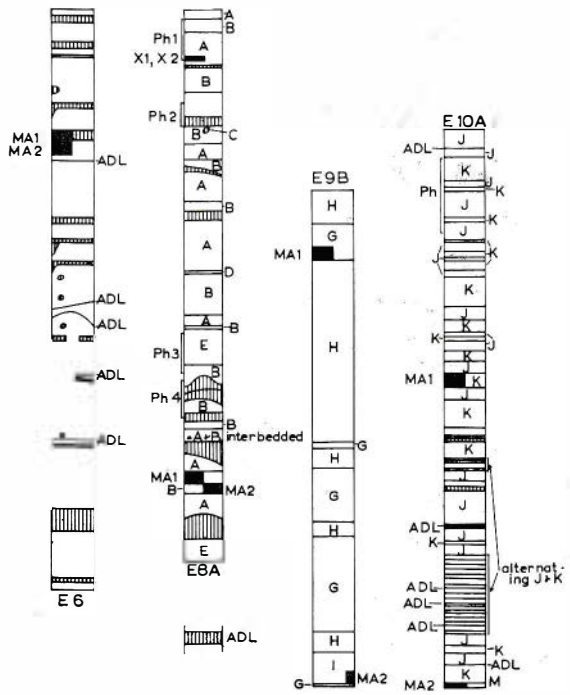

VERTICAL SCALE: 35.4 mm = 1 m

FIG. 8. Stratigraphy of cores E6, E8A, E9B, and E10A.

E6: Pale olive mud with adiatelic layers of laminated silt or muddy silt (turbidites) and pockets of silt (disrupted turbidites). The silt is grey to pale grey, but acquires an olive chroma as the clay content rises.

E8A: Mud with forams, pale olive (A) to very pale olive (B), with adiatelic layers of laminated silt or muddy silt (turbidites) and pockets of silt (disrupted turbidites). The silt is grey to pale grey, but acquires an olive chroma as the clay content rises. There also occur (i) a conspicuous paramictic zone (E) consisting of silt, muddy silt, silty mud, and mud, varying in colour from grey (silt) to pale olive (mud); and (ii) a thin layer of pale grey mud (D). X1 is a pale alteration burrow; X2 is the matrix of the burrow. (*The sixth layer down, below the* (B) *layer, is* (A).)

E9B: (G) pale sub-olive mud (with subordinate moderately sandy mud), containing (H) the same but very pale olive; near the base there occurs a layer (I) of white silt, consisting almost entirely of pumice.

E10A: (J) pale olive to very pale olive mud or moderately sandy mud with numerous relatively sandy layers (K), many with muddy aggregates. There also occur a number of thin adiatelic layers, consisting of muddy very sandy silt, often laminated and with concentrations of mud pellets or pumice. At the base there is a layer (M) of white pumiceous silt.

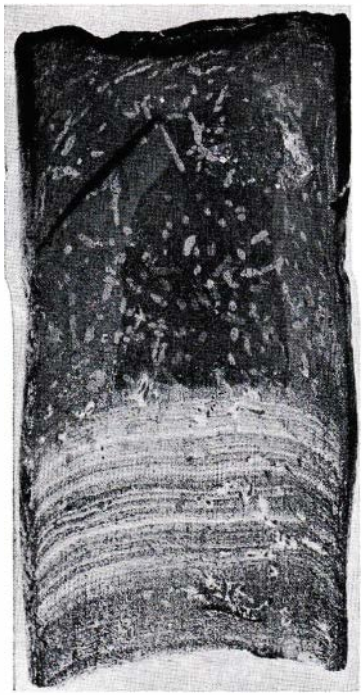

FIG. 9.

FIG. 9. Core E8A, section Ph2 (photographed when damp). The band forming the lower part of the core section is a turbidite consisting of laminated muddy silt (pale sub-olive when dry). This layer is overlain by mud (pale olive when dry) with a dark sulphide-bearing zone in the centre. The mud contains numerous pale alteration burrows, several of which show miomelanosis in the central zone. Equivalent burrows occur in the turbidite band but these consist of a predominantly silty outer layer enclosing a muddy centre with a much smaller proportion of silt. (*Actual size*)

FIG. 10.

FIG. 10. Core E8D, section Ph2 (photographed when damp). The lower layer consists of mud (very pale olive when dry) with a dark sulphide-bearing zone in the centre. This portion is overlain by a turbidite band of laminated silt (grey). The turbidite is overlain by mud (pale sub-olive when dry). The main flat surface on the specimen lies in the plane of the photograph, but because of the friable state of the material, it was necessary to bevel the upper edge of the specimen. The small bevelled surface shows the upper contact of the turbidite. (*Actual size*)

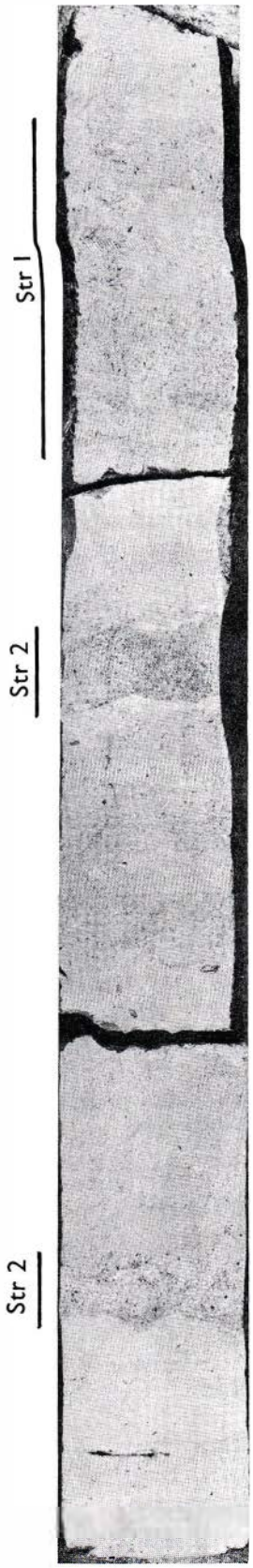

FIG. 11.

FIG. 11. Core E10A, section Ph (photographed when dry). Pale olive mud containing sandy layers with aggregates. A group of these layers (Str 1) occurs near the top of the section, while two very distinct but more isolated layers (Str 2) occur lower down. These layers contain muddy faecal pellets and show grain-size mottling. ($\frac{3}{4}$ *actual size*)

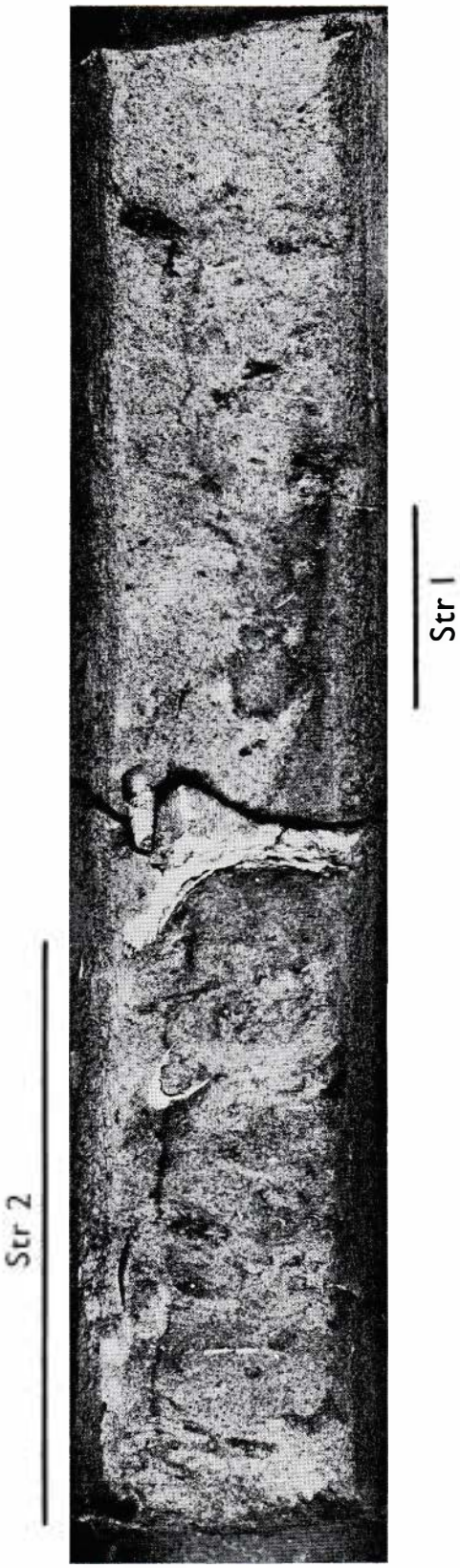

FIG. 12.

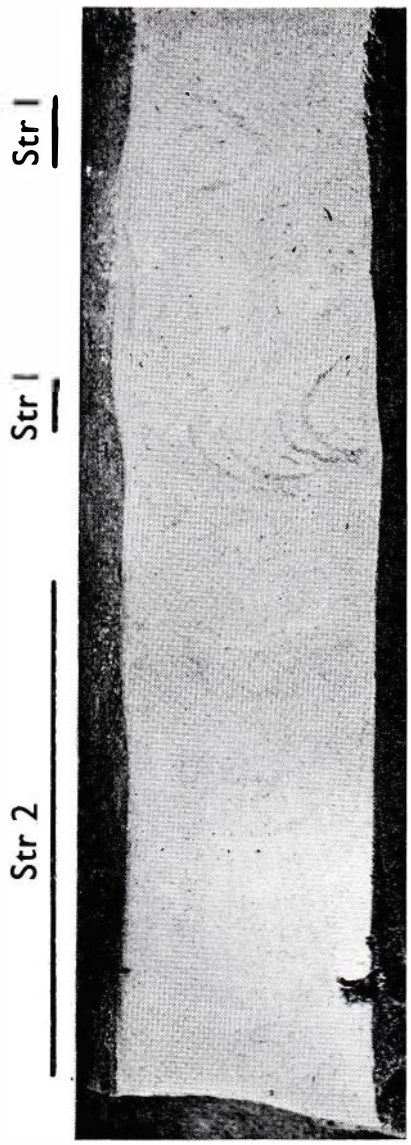

FIG. 13.

FIG. 12. Core A796, section Ph3 (photographed when dry). Pale olive very muddy sand with shells and shell fragments showing sandy relict burrows (Str 1) and a zone with faint banding and lamination (Str 2). (*Actual size*)

FIG. 13. Core E3A, section Ph (photographed when dry). Pale olive mud showing meniscus burrows (Str 1) and lamination (Str 2.) (*Actual size*)

Calvert and Veevers 1962 (fig. 2): terrigenous sediment from the north-west slope of the Timor Trough;

Coleman, Gagliano, and Webb 1964 (plates I–IV): sediments from the Mississippi Delta;

Ericson, Ewing, Heezen, and Wollin 1955 (plate 2, fig. 3): pelagic lutite with a calcareous turbidite layer from the Puerto Rico Trench;

Ewing, Ericson and Heezen, 1958 (fig. 26): lutites interbedded with silty turbidites from the Gulf of Mexico;

Gorsline and Emery 1959 (plate 1): lutites interbedded with sandy and silty turbidites from basins off California;

Hulsemann and Emery, 1961 (plate 2): lutites from a basin (Santa Barbara) off California.

Moore and Scruton 1957 (figs 3, 4, 16): terrigenous sediments from the Mississippi Delta, and from coastal waters off central Texas;

Pantin 1965 (plate I): sand and sandy silt from a New Zealand fiord;

Riedel and Funnell 1964 (plate 14, core CAP 5 BP, and plate 15, core DWBG 11): pelagic sediments from the Pacific Ocean.

Ryan and Heezen 1965 (plate 4, A and C): lutites interbedded with sandy and silty turbidites from the Ionian Sea;

van Straaten 1959 (figs 1, 4, 6, 10, 20–21, 23–24): terrigenous shallow-water sediments from the Netherlands and the Rhône Delta;

The literature also contains numerous examples of lamination in unconsolidated marine sediments. These references include:

Allen 1965 (plates 1F, 3A, 4D and G, 5B, C and E): sediments from the Niger Delta;

Arrhenius 1952 (plate 2.6.5, core 61); pelagic sediment from the east Pacific Ocean.

Bouma 1964 (figs 12–17): terrigenous sediments from canyons off California and Baja California;

Bouma 1965 (figs 3, 4, 9, 12, 16): terrigenous sediments from canyons off California and Baja California:

Calvert and Veevers 1962 (figs 1, 2, 4, 5): terrigenous sediments from tidal flats (near the Colorado River Delta), from the Timor Trough, and from the central Gulf of California;

Coleman, Gagliano, and Webb 1964 (plates I–IV): sediments from the Mississippi Delta;

Ericson, Ewing, Heezen, and Wollin 1955 (plate 2, fig. 3): pelagic lutite with a calcareous turbidite layer from the Puerto Rico Trench;

Ewing, Ericson, and Heezen 1958 (fig. 26): lutites interbedded with silty turbidites from the abyssal plain in the Gulf of Mexico;

Gorsline and Emery 1959 (plate 1): lutites interbedded with sandy and silty turbidites from basins off California;

Greenman and LeBlanc 1956 (fig. 3, core 510; fig. 6, cores 149, 549): terrigenous sediments from the shelf and the abyssal plain in the Gulf of Mexico;

Hulsemann and Emery, 1961 (plate 2): lutites from a basin (Santa Barbara) off California;

Moore and Scruton, 1957 (figs 3, 4, 16): terrigenous sediments from the Mississippi Delta, and from coastal waters off central Texas;

Pantin 1966 (plate 2a and b): terrigenous sediments from the shelf in Hawke Bay, New Zealand;

Riedel and Funnell 1964 (plate 14, core CAP 5 BP): pelagic sediments from the Pacific Ocean;

Ryan and Heezen 1965 (plate 4, A and C): lutites interbedded with sandy and silty turbidites from the Ionian Sea;

Shepard and Einsele 1962 (plate I, figs 1, 2, 4, 5; plate II, figs 1, 2, 4, 5, 6): lutites and sandy turbidites from a trough (San Diego) off California;

van Straaten 1959 (figs 1, 3, 4–6, 9–11, 19, 23–4): terrigenous shallow-water sediments from the Netherlands, northwest Germany, and the Rhône Delta.

Transition Planes (figs 15, 16, and 17)

It is convenient to use this term for abrupt vertical changes in the character of the sediments whether or not there is an erosional break at the junction. For brevity the expression "T-plane" will be used. A T-plane with an erosional break would be a disconformity, but it is possible to have disconformities with no change in the type of sediment, just as it is possible to have an abrupt change in the type of sediment without any break in deposition.

Several T-planes occur in the present area, being found in A792 (canyon), A795 (shelf), A807 (upper slope), A808 (slope high), and A809 (slope high).

The lower part of A792 consists of grey mud with occasional pebbles, changing abruptly to pale olive pebbly very sandy mud about 60 cm below the top of the core (fig. 16). The nature of this T-plane will be discussed later in connection with "creep-slumping", a process which has affected the sediments in this core.

The lower part of A795 consists of moderately sandy mud (pale grey) changing abruptly to very sandy mud (pale olive) about 64 cm from the top of the core (fig. 17). There is no evidence of erosion at the junction. The sand fractions in the upper and lower parts of the core are very similar, indicating that there was no significant change in current strength corresponding to the T-plane. The sharp decrease in the proportion of mud points to a reduction in the supply of muddy detritus in the environment, a change which may have occurred

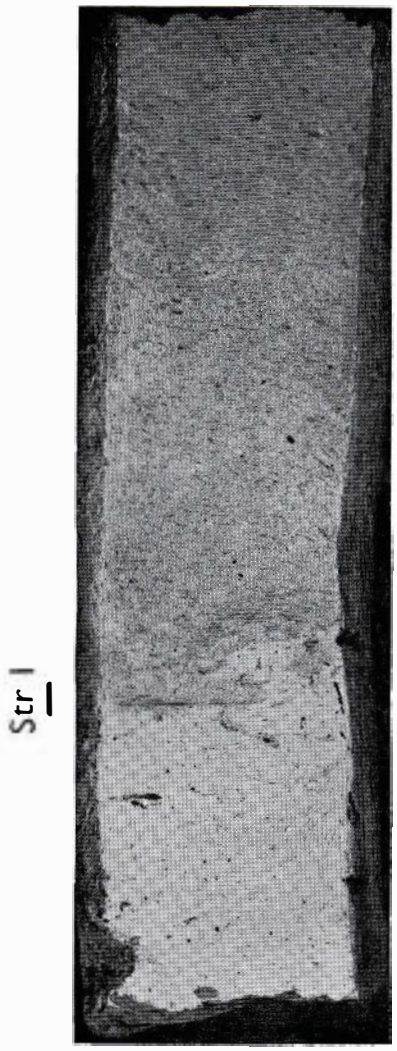

FIG. 15.

FIG. 15. Core A807, section Ph2 (photographed when dry). T-plane (Str 1) separating pale grey mud (below) from pale olive mud (above). (*Actual size*)

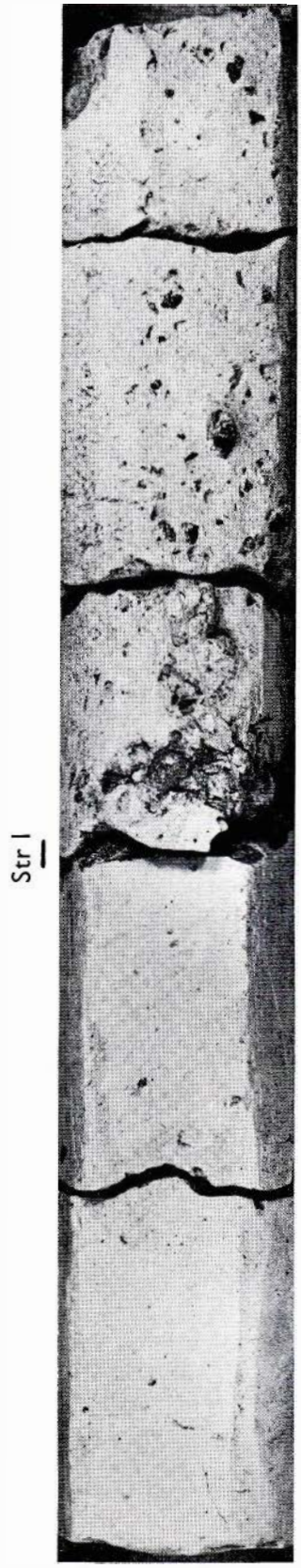

FIG. 16.

FIG. 16. Core A792, section Ph (photographed when dry). Grey mud with occasional pebbles (below), separated by a T-plane (Str 1) from pale olive pebbly very sandy mud (above). The pebbles in these sediments have probably been transported by creep-slumping: those below the T-plane are friable and weathered brown. ($\frac{3}{4}$ *actual size*)

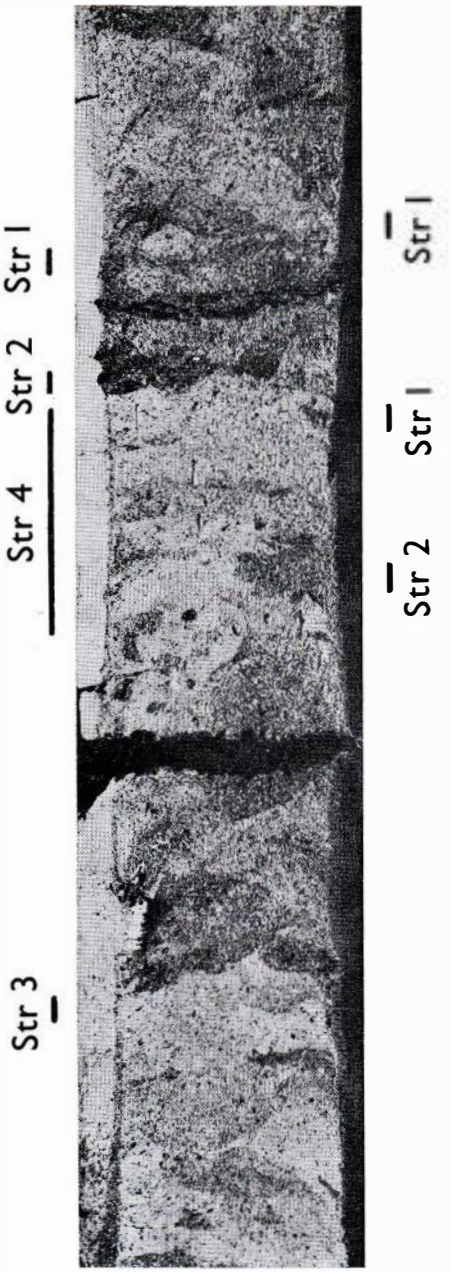

FIG. 17. Core A795, section Ph2 (photographed when dry). Below the T-plane (Str 3), the core section consists of pale grey moderately sandy mud; the same type of sediment forms a layer (Str 4) a short distance above. The remainder of the core section consists of pale olive very sandy mud. Numerous organic structures are visible: muddy burrows (Str 1); sandy relict burrows (Str 2); and sandy infilled burrows with muddy walls immediately below Str 4. (*Actual size*)

as a result of the Holocene rise in sea level slowing down. While sea level was still rising coastal wave action would be continually attacking the cliffs in the area, which consist partly of easily eroded Tertiary mudstones. This would release large quantities of mud into the sea. When the rise in sea level halted, however, an armouring belt of coarse sediment would be quickly built up and cliff erosion would almost cease. A slight further transgression may be indicated in A795 by a thin band of pale grey moderately sandy mud just above the base of the very sandy mud. The reason for the sudden change of colour at the T-plane in A795 is discussed on p. 37.

A809 occurs on the upper part of a morphologic high, situated on the continental slope, and contains two well marked T-planes. The lowest part of the core consists of pale grey mud with virtually no sand. Above this comes pale sub-olive to grey moderately sandy mud with numerous mud pellets some of which are slightly glauconitic. At the top of the core comes pale olive, very sandy mud with numerous glauconitic grains. Sharp contacts occur between the three main units and each of the two lower units contains infilled burrows of material similar to that of the overlying unit.

The lower T-plane is clearly a disconformity and may represent a considerable time interval. The deposition of sand-free mud at this locality is difficult to explain in terms of any reasonable assumptions about currents and sediment supply, in view of the much higher proportion of sand in the overlying layers. It is therefore probable that the sand fraction has been virtually removed from the lowest layer by diagenetic reactions involving solution of sand grains. The few sand grains which do occur in the sediment are frosted and pitted, supporting the view that they have been corroded as a result of chemical reactions during diagenesis. This removal of sand must have occurred before the deposition of the overlying layer, since material similar to the latter forms infilled burrows in the sand-free mud. It is thus probable that the sand-free mud is considerably older than the overlying layer.

The disconformity at the top of the sand-free mud must represent at least two changes in the magnitude or direction of the currents in the area. The first change, involving erosion, was evidently caused by an increase in average current velocity at the locality of A809; this does not necessarily imply an increase in velocity over the whole area, but only that the current pattern shifted in such a way as to raise the current velocity around A809. The second change, resulting in the deposition of moderately sandy mud, probably represents a reduction in local current velocity. The abundance of mud pellets shows that some muddy formation (probably the sand-free mud or its mechanical equivalent) was being eroded. However, the glauconitised character of some of the mud pellets shows that they sometimes remained on the sea bed for a considerable time without significant lateral transport.

Calvert and Veevers 1962 (fig. 2): terrigenous sediment from the north-west slope of the Timor Trough;

Coleman, Gagliano, and Webb 1964 (plates I–IV): sediments from the Mississippi Delta;

Ericson, Ewing, Heezen, and Wollin 1955 (plate 2, fig. 3): pelagic lutite with a calcareous turbidite layer from the Puerto Rico Trench;

Ewing, Ericson and Heezen, 1958 (fig. 26): lutites interbedded with silty turbidites from the Gulf of Mexico;

Gorsline and Emery 1959 (plate 1): lutites interbedded with sandy and silty turbidites from basins off California;

Hulsemann and Emery, 1961 (plate 2): lutites from a basin (Santa Barbara) off California.

Moore and Scruton 1957 (figs 3, 4, 16): terrigenous sediments from the Mississippi Delta, and from coastal waters off central Texas;

Pantin 1965 (plate I): sand and sandy silt from a New Zealand fiord;

Riedel and Funnell 1964 (plate 14, core CAP 5 BP, and plate 15, core DWBG 11): pelagic sediments from the Pacific Ocean.

Ryan and Heezen 1965 (plate 4, A and C): lutites interbedded with sandy and silty turbidites from the Ionian Sea;

van Straaten 1959 (figs 1, 4, 6, 10, 20–21, 23–24): terrigenous shallow-water sediments from the Netherlands and the Rhône Delta;

The literature also contains numerous examples of lamination in unconsolidated marine sediments. These references include:

Allen 1965 (plates 1F, 3A, 4D and G, 5B, C and E): sediments from the Niger Delta;

Arrhenius 1952 (plate 2.6.5, core 61); pelagic sediment from the east Pacific Ocean.

Bouma 1964 (figs 12–17): terrigenous sediments from canyons off California and Baja California;

Bouma 1965 (figs 3, 4, 9, 12, 16): terrigenous sediments from canyons off California and Baja California:

Calvert and Veevers 1962 (figs 1, 2, 4, 5): terrigenous sediments from tidal flats (near the Colorado River Delta), from the Timor Trough, and from the central Gulf of California;

Coleman, Gagliano, and Webb 1964 (plates I–IV): sediments from the Mississippi Delta;

Ericson, Ewing, Heezen, and Wollin 1955 (plate 2, fig. 3): pelagic lutite with a calcareous turbidite layer from the Puerto Rico Trench;

Ewing, Ericson, and Heezen 1958 (fig. 26): lutites interbedded with silty turbidites from the abyssal plain in the Gulf of Mexico;

Gorsline and Emery 1959 (plate 1): lutites interbedded with sandy and silty turbidites from basins off California;

Greenman and LeBlanc 1956 (fig. 3, core 510; fig. 6, cores 149, 549): terrigenous sediments from the shelf and the abyssal plain in the Gulf of Mexico;

Hulsemann and Emery, 1961 (plate 2): lutites from a basin (Santa Barbara) off California;

Moore and Scruton, 1957 (figs 3, 4, 16): terrigenous sediments from the Mississippi Delta, and from coastal waters off central Texas;

Pantin 1966 (plate 2a and b): terrigenous sediments from the shelf in Hawke Bay, New Zealand;

Riedel and Funnell 1964 (plate 14, core CAP 5 BP): pelagic sediments from the Pacific Ocean;

Ryan and Heezen 1965 (plate 4, A and C): lutites interbedded with sandy and silty turbidites from the Ionian Sea;

Shepard and Einsele 1962 (plate I, figs 1, 2, 4, 5; plate II, figs 1, 2, 4, 5, 6): lutites and sandy turbidites from a trough (San Diego) off California;

van Straaten 1959 (figs 1, 3, 4–6, 9–11, 19, 23–4): terrigenous shallow-water sediments from the Netherlands, northwest Germany, and the Rhône Delta.

Transition Planes (figs 15, 16, and 17)

It is convenient to use this term for abrupt vertical changes in the character of the sediments whether or not there is an erosional break at the junction. For brevity the expression "T-plane" will be used. A T-plane with an erosional break would be a disconformity, but it is possible to have disconformities with no change in the type of sediment, just as it is possible to have an abrupt change in the type of sediment without any break in deposition.

Several T-planes occur in the present area, being found in A792 (canyon), A795 (shelf), A807 (upper slope), A808 (slope high), and A809 (slope high).

The lower part of A792 consists of grey mud with occasional pebbles, changing abruptly to pale olive pebbly very sandy mud about 60 cm below the top of the core (fig. 16). The nature of this T-plane will be discussed later in connection with "creep-slumping", a process which has affected the sediments in this core.

The lower part of A795 consists of moderately sandy mud (pale grey) changing abruptly to very sandy mud (pale olive) about 64 cm from the top of the core (fig. 17). There is no evidence of erosion at the junction. The sand fractions in the upper and lower parts of the core are very similar, indicating that there was no significant change in current strength corresponding to the T-plane. The sharp decrease in the proportion of mud points to a reduction in the supply of muddy detritus in the environment, a change which may have occurred

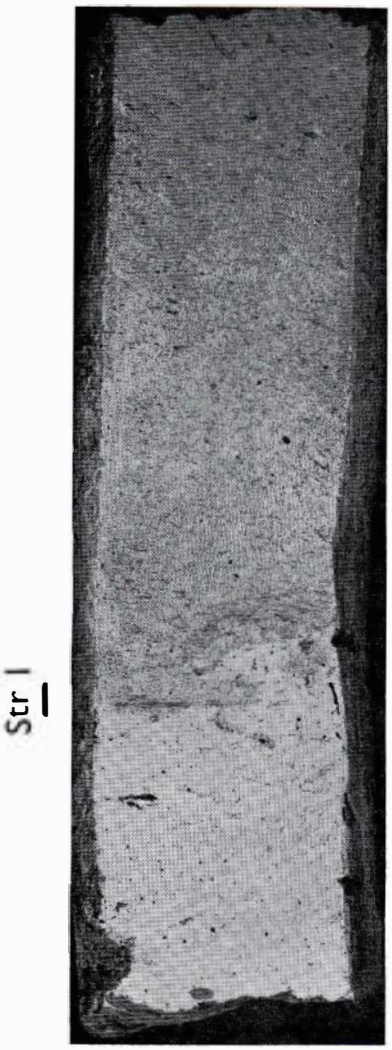

FIG. 15.

FIG. 15. Core A807, section Ph2 (photographed when dry). T-plane (Str 1) separating pale grey mud (below) from pale olive mud (above). (*Actual size*)

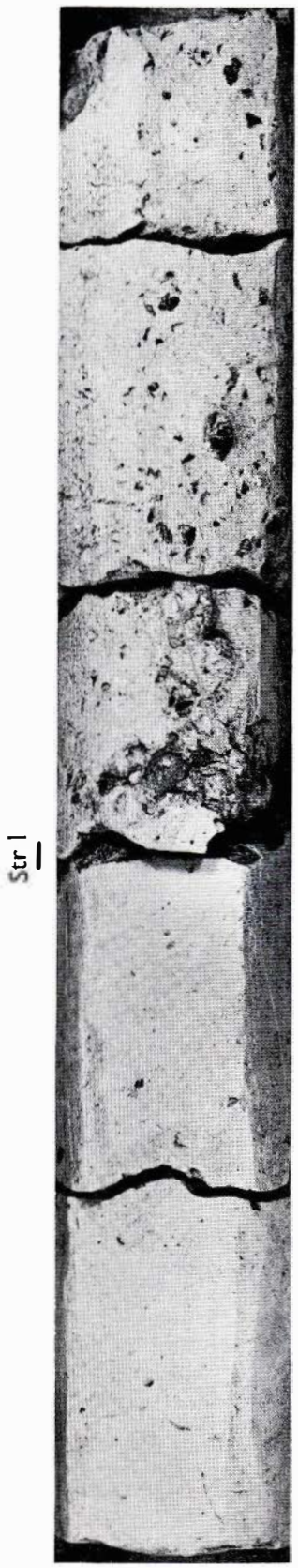

FIG. 16.

FIG. 16. Core A792, section Ph (photographed when dry). Grey mud with occasional pebbles (below), separated by a T-plane (Str 1) from pale olive pebbly very sandy mud (above). The pebbles in these sediments have probably been transported by creep-slumping: those below the T-plane are friable and weathered brown. (¾ *actual size*)

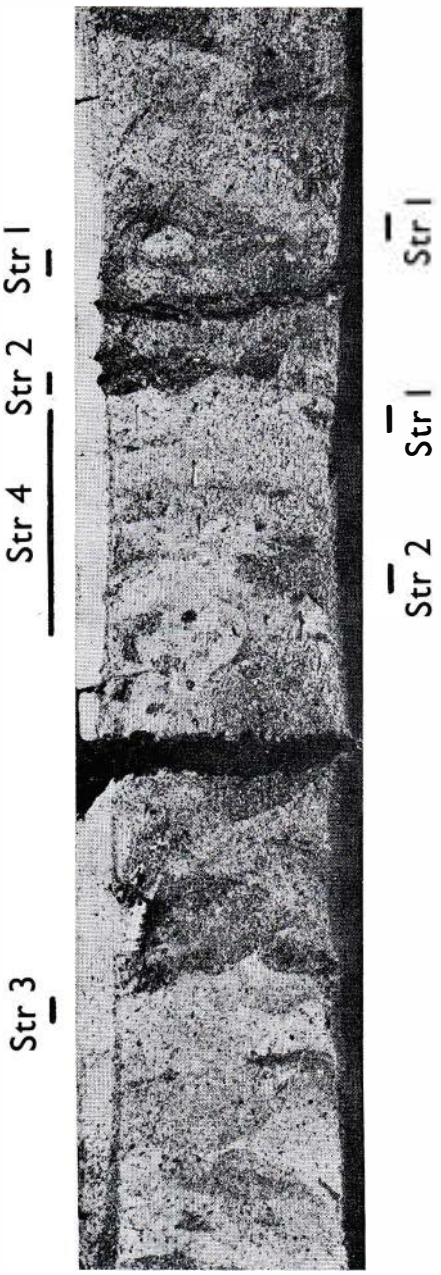

FIG. 17. Core A795, section Ph2 (photographed when dry). Below the T-plane (Str 3), the core section consists of pale grey moderately sandy mud; the same type of sediment forms a layer (Str 4) a short distance above. The remainder of the core section consists of pale olive very sandy mud. Numerous organic structures are visible: muddy burrows (Str 1); sandy relict burrows (Str 2); and sandy infilled burrows with muddy walls immediately below Str 4. (*Actual size*)

as a result of the Holocene rise in sea level slowing down. While sea level was still rising coastal wave action would be continually attacking the cliffs in the area, which consist partly of easily eroded Tertiary mudstones. This would release large quantities of mud into the sea. When the rise in sea level halted, however, an armouring belt of coarse sediment would be quickly built up and cliff erosion would almost cease. A slight further transgression may be indicated in A795 by a thin band of pale grey moderately sandy mud just above the base of the very sandy mud. The reason for the sudden change of colour at the T-plane in A795 is discussed on p. 37.

A809 occurs on the upper part of a morphologic high, situated on the continental slope, and contains two well marked T-planes. The lowest part of the core consists of pale grey mud with virtually no sand. Above this comes pale sub-olive to grey moderately sandy mud with numerous mud pellets some of which are slightly glauconitic. At the top of the core comes pale olive, very sandy mud with numerous glauconitic grains. Sharp contacts occur between the three main units and each of the two lower units contains infilled burrows of material similar to that of the overlying unit.

The lower T-plane is clearly a disconformity and may represent a considerable time interval. The deposition of sand-free mud at this locality is difficult to explain in terms of any reasonable assumptions about currents and sediment supply, in view of the much higher proportion of sand in the overlying layers. It is therefore probable that the sand fraction has been virtually removed from the lowest layer by diagenetic reactions involving solution of sand grains. The few sand grains which do occur in the sediment are frosted and pitted, supporting the view that they have been corroded as a result of chemical reactions during diagenesis. This removal of sand must have occurred before the deposition of the overlying layer, since material similar to the latter forms infilled burrows in the sand-free mud. It is thus probable that the sand-free mud is considerably older than the overlying layer.

The disconformity at the top of the sand-free mud must represent at least two changes in the magnitude or direction of the currents in the area. The first change, involving erosion, was evidently caused by an increase in average current velocity at the locality of A809; this does not necessarily imply an increase in velocity over the whole area, but only that the current pattern shifted in such a way as to raise the current velocity around A809. The second change, resulting in the deposition of moderately sandy mud, probably represents a reduction in local current velocity. The abundance of mud pellets shows that some muddy formation (probably the sand-free mud or its mechanical equivalent) was being eroded. However, the glauconitised character of some of the mud pellets shows that they sometimes remained on the sea bed for a considerable time without significant lateral transport.

The upper T-plane in A809 is also clearly a disconformity and must likewise correspond to two successive changes in the current regime. There was evidently an increase in local current velocity causing erosion at the top of the moderately sandy mud followed by a decrease in current velocity resulting in the deposition of glauconitic very sandy mud. The lower proportion of mud in this layer may be due to the covering-over of the source bed which provided the mud pellets in the underlying layer. The reason for the sudden changes of colour at the T-planes in A809 is discussed on p. 37.

A808 occurs on the same slope high as A809 and contains two T-planes. About 26 cm below the top of the core, massive mud gives way to mud which becomes friable and develops numerous irregular cracks when allowed to dry out. This section evidently consists of accumulated, poorly defined, small mud lumps. At the top of the core the "friable" mud gives way to a mud consisting of well defined mud lumps, many of which are glauconitised. This uppermost layer becomes incoherent when dry.

The lower T-plane is probably a major disconformity, and may well be equivalent to the lower T-plane in A809. The upper T-plane is probably a plane of mechanical and chemical diagenesis representing the depth to which the matrix between the mud lumps has been partly washed out by currents and the mud lumps glauconitised.

A807 shows an abrupt transition from pale grey and pale sub-olive mud below to pale olive mud above (fig. 15). The lack of change in grain size at the T-plane, together with the location of A807 on the upper slope indicates that the T-plane is a disconformity produced not by erosion, but as a result of slumping. It is unlikely that in a uniformly deposited sediment the chemical changes involved in converting olive mud to grey mud would occur along a sharp boundary. These changes are probably spread over a transition zone at least 10–15 cm thick such as in E13. Evidently the grey mud below the T-plane was originally overlain by at least 10–15 cm of similar or transitional material which has been mechanically removed. The most probable explanation is that a slump removed the sediment above the T-plane after which deposition continued in the form of olive mud. The change from olive to grey mud occurs during progressive burial, but in the present case the olive mud above the T-plane has not been buried to a sufficient depth for the change to begin.

Although fossil sediments very often contain T-planes, the literature gives relatively few references to structures of this type in unconsolidated marine sediments. The available references include:

Allen 1965 (plate 4A and D): sediments from the Niger Delta;

Ericson, Ewing, and Wollin 1964 (fig. 4): lutites from the Arctic Ocean;

Greenman and LeBlanc 1956 (fig. 3, core 504; fig. 6, cores 341, 339): sediments from the shelf and the abyssal plain in the Gulf of Mexico; the sediments in these cores are dominantly terrigenous, although calcareous biogenic material occurs in core 504 (from the shelf);

Riedel and Funnell 1964 (plate 14, core CAP 5 BP; plate 23, core MSN 150 G): pelagic sediments from the Pacific Ocean;

Shepard and Einsele 1962 (plate II, fig. 7; plate III, fig. 3): terrigenous sediments from a trough (San Diego) off California.

Paramictic Structures (figs 18–22)

The general term "paramictic structures" is proposed here for any type of structure formed in sediments which have suffered penecontemporaneous inorganic disturbance of moderate intensity, involving distortion of bedding. The corresponding process will be called "paramixis". These general terms are intended to cover the results of slumping, earthquakes, internal convection, or any other inorganic agency. The terms are restricted, however, to beds in which the remains of original sedimentary units can still be identified in spite of disintegration and flowage. Fossil sediments containing structures of this type have been called "fragmented beds" by Wood and Smith (1958, p. 172).

The term "fragmented" is not entirely suitable, since it places too much emphasis on the quasi-solid behaviour of some of the sedimentary units. "Paramixis", on the other hand, may be applied to quasi-solid, hydroplastic, or quasi-liquid behaviour. Heavily disturbed beds, containing virtually no relict structures, are not covered by "paramixis". The term "slurried" has been applied to beds in this condition by Wood and Smith (1958, p. 173) and Elliott (1965, fig. 1).

In the present area paramixis is found only on the lower part of the slope and in the trench, being very conspicuous in some of the turbidite cores. The structures take the form of highly distorted bedding associated with a mechanical mixture containing fragments of local sedimentary units. Individual fragments range from a few millimetres to a few centimetres in width and vary considerably in shape. The more rigid fragments show blocky outlines with sharp edges and bedding either undistorted or bent into simple flexures; this type of structure characterises the more sandy or silty units. The more plastic fragments (typically containing a high proportion of clay-size material) take the form of pods, pennants, or stringers, in which the boundaries may be somewhat diffuse and the bedding is highly distorted or even obliterated. Lithological contacts usually possess moderate or high dips. Zones with paramixis are typically 20–30 cm thick; and are separated by beds showing little or no evidence of disturbance.

Although the disturbed material normally shows little evidence of ordered structures, diapiric structure is occasionally seen in the turbidite layers. The general lack of order may only be apparent, for the cores are only 5 cm wide and any significantly larger structures would escape detection.

In some parts of the cores, paramixis is so conspicuous that the possibility of disruption by the coring process must be considered. The proximity of paramictic zones and virtually undisturbed beds shows that the cores are not grossly distorted, but it is still possible for mechanically sensitive beds to be preferentially disturbed by coring without destruction of the essential stratigraphy of the core. One possible criterion for distinguishing between natural and artificial paramixis is that structures produced by coring would tend to have an axis (or plane) of symmetry coinciding approximately with the geometrical axis of the core. On this basis, it appears that the small diapiric structures (fig. 14) are probably due to coring disturbance, but the remainder of the paramictic structures, which do not show this type of symmetry, are the result of natural processes.

Theoretically, paramixis could originate in several different ways. In the present area the principal causes of paramixis appear to be (i) slumping and (ii) gravitational adjustment (convection) between layers of different densities. These processes will be called respectively "slumping paramixis" or "paramictic slumping," and "convective paramixis." Evidence for slumping paramixis can be seen in two portions of E12 where asymmetrically distorted beds show that lateral movement has taken place (figs 18 and 19). On the other hand, the widespread occurrence of steep-dipping contacts (fig. 20) provide good evidence for movement with a strong vertical component, indicating convective paramixis. In a number of cases, the paramictic structures provide no clear evidence of their origin (figs 21 and 22); some of these undifferentiated structures are presumably due to slumping and others to convection.

Consideration of the properties of the turbidites and the associated mud shows that convective re-adjustment is inherently probable.

A basic difference in density must result from the difference in mechanical composition between the two types of sediment. The water content of the mud, when originally deposited, would probably have been sufficient to cause the density to be less than in the turbidite layers. The rapid deposition of a turbidite on top of the soft mud might thus cause convective re-adjustment, with the silty layer breaking up and sinking a few centimetres into the mud. The difference in behaviour of the muddy and silty units during paramixis is presumably due to a relative lack of cohesion in the silt compared with that in the mud.

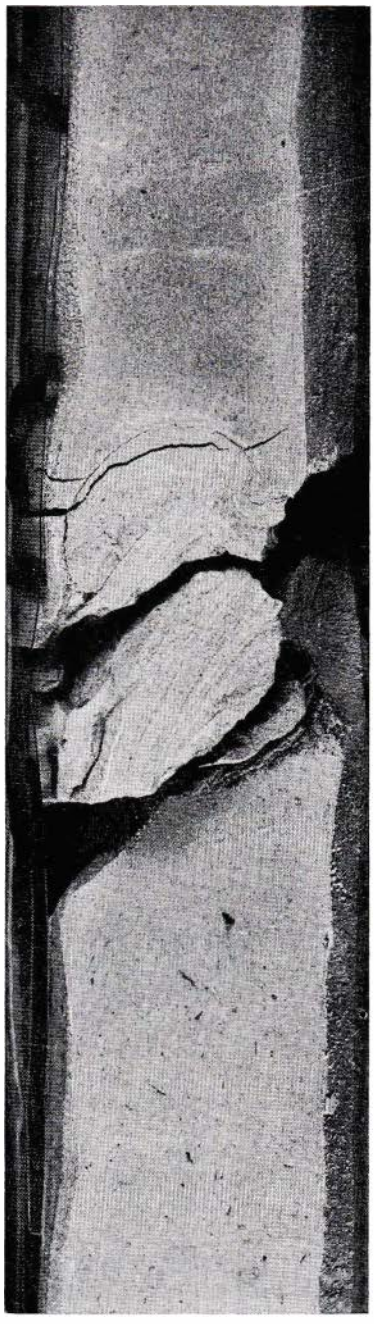

FIG. 18. Core E12, section Ph3 (photographed when dry). Disrupted and dismembered turbidite layer of laminated silt (pale grey) overlain by an asymmetrically distorted turbidite layer consisting of interlaminated muddy silt and mud (overall colour pale sub-olive). The turbidite layers are underlain by mud (pale olive), and overlain by silty mud (sub-olive). The structure of the turbidite layers is probably due to paramictic slumping. (*Actual size*)

Slightly deeper and more compacted mud, on the other hand, might well be denser than the adjacent turbidites. In such a situation, a turbidite would tend to break up and rise through the mud towards the surface.

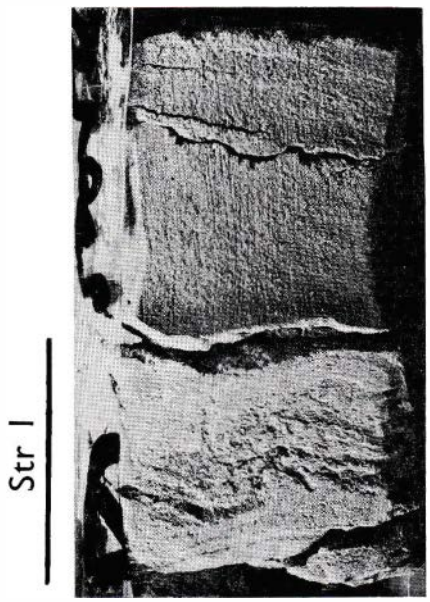

FIG. 19.

FIG. 19. Core E12, section Ph1 (photographed when dry). Thin silty turbidite layers (Str 1) showing asymmetric distortion probably due to paramictic slumping. These turbidites (mainly pale grey) are overlain by a band of pale olive mud, the upper part of which contains a few very thin silty turbidites. (*Actual size*)

FIG. 20. Core E8A, section Ph3 (photographed when dry). Paramictic zone containing silt, muddy silt, silty mud, and mud, the colour varying from grey (silt) to pale olive (mud); paramixis probably convective. (*Actual size*)

FIG. 20.

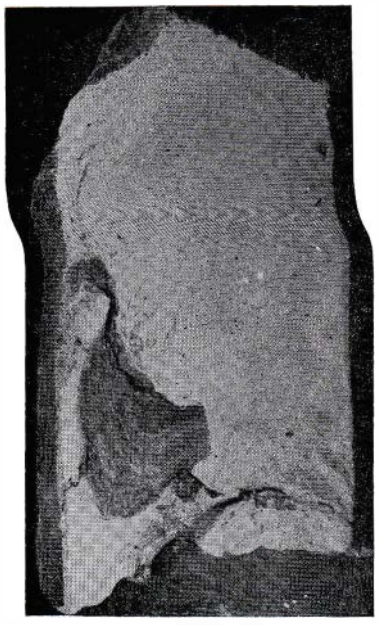

FIG. 21.

FIG. 21. Core E12, section Ph2 (photographed when dry). A typical fragment of a disrupted turbidite bed, consisting of grey silt with distorted lamination, enclosed in a matrix of pale olive mud. The type of paramixis involved is not certain, although convection is more probable than slumping. (*Actual size*)

FIG. 22.

FIG. 22. Core E8D, section Ph1 (photographed when damp). A fragment of a disrupted turbidite bed (Str 1), consisting of grey to pale grey silt, occurs at the top of the core section. Paramixis is probably convective. This turbidite fragment is embedded in mud (pale olive when dry) containing a remnant of a very dark sulphide-bearing zone (Str 2). The middle part of the core section consists of mud (very pale olive when dry), with a higher proportion of forams than the material above and below: faint grain-size mottling is visible. The lower part of the core section consists of mud (pale sub-olive when dry) with a poorly-developed sulphide-bearing zone (Str 3). In the centre of this zone there is a near-vertical burrow (Str 4): the outer part of this structure has the appearance of a pale alteration burrow and shows miomelanosis, while the inner part is much darker and shows meniscus structure. (This burrow is slightly sinuous, resulting in two separated oblique sections). Towards the base of the core section, there is a pale alteration burrow (Str 5) which shows miomelanosis where it meets the central sulphide-bearing zone. (*85% actual size*)

Although paramixis could occur spontaneously whenever density differences between adjoining layers were sufficient, it could also occur in response to seismic vibrations, particularly if the muddy layers behaved in a thixotropic manner. The relative importance of spontaneous and earthquake-induced paramixis cannot be decided without further information.

Paramixis would also be accentuated by the expulsion of water from compacting sediments. Experiments made by Dangeard *et al.* (1964, pp. 5936–7) and mentioned by Kuenen (1965, p. 24 and fig. 4) indicate that the expelled water is not distributed uniformly through the overlying sediment, but is concentrated in local channels of upwelling. Paramixis would be assisted by the upward passage of water through these channels.

Kuenen (1965, figs 8, 9, and 10) has described convective sedimentary structures, in both fossil sediments and experimental material, which are very similar in appearance to the convective paramictic structures in the present area. In the same paper Kuenen (loc. cit., fig. 6) illustrates an experimental slump accompanied by paramictic structures; the numerous steep-dipping contacts in the upper part of the sediment may indicate that the slump was associated with some convection.

The occurrence of cores with abundant paramixis (for instance E12) not far from cores of similar material with little or no paramixis (for instance E6) indicates that local conditions have a considerable influence on the formation of paramictic structures. Possibly a high local gradient with incipient slumping, or the presence of a nearby water expulsion channel, would facilitate paramixis.

According to Elliott's classification of subaqueous structures (1965, fig. 1), the paramictic structures in the present area would fall into the "endokinematic vertical transposition" or the "endokinematic horizontal transposition" categories. The sediment behaviour varies from quasi-liquid to quasi-solid.

The literature on fossil sediments contains numerous descriptions of structures which appear to be due to convective paramixis. These references include:

Davies 1965 (plates I–III): Carboniferous shallow-water sandstones in Yorkshire, England;

Pettijohn and Potter 1964 (plates 106A, 106B, 112A): Tertiary flysch from Italy, Krosno Beds (Oligocene) from Poland, and Pennsylvanian sandstone and siltstone from the U.S.A.;

Wood and Smith 1958 (text fig. 6; plate VI, fig. 4): Silurian greywackes and mudstones in Wales.

Unconsolidated marine (and lacustrine) sediments also contain structures which are probably due, partly or wholly, to convective paramixis. Some of these structures, however, are less easily identified than the fossil examples, because of the limited size of cores or box-grab samples as compared with rock outcrops. References to probable convective paramixis in unconsolidated sediments include:

Bouma 1964 (fig. 5, point 53): terrigenous sediment from the central Gulf of California.

Bouma 1965 (fig. 14, upper part): terrigenous sediment from a canyon off Baja California.

Ewing, Ericson, and Heezen 1958 (fig. 27*): highly disturbed layer in pelagic sediments from the Gulf of Mexico. The varied age and lithology of the sedimentary components show that this layer was formed as a result of a slump: however, the prevalence of contorted steep-dipping contacts indicates that convective paramixis has occurred at a later stage;

Shepard and Einsele 1962 (plate I, fig. 3): terrigenous sediments from a trough (San Diego) off California.

Smith, 1959 (fig. 4, central part): lacustrine silts and clays from Windermere, England.

The literature also contains numerous descriptions of structures which are apparently due to paramictic slumping. These structures are found in both unconsolidated marine (and lacustrine) sediments and fossil sediments. References include:

Bouma 1964 (fig. 3, upper part; fig. 5, point 52; fig. 7, point 47; fig. 17, point 50): terrigenous sediments from the central Gulf of California, and from canyons off California and Baja California;

Bouma 1965 (fig. 16, point 21; fig. 17, point 27): terrigenous sediments from canyons off California and Baja California;

Smith 1959 (figs 3 and 4): silts and clays from Windermere, England;

Wood and Smith 1958 (plate VIII, fig. 3): Silurian greywackes and mudstones in Wales.

Non-paramictic Structures Associated with Slumping

In the present area two basic types of slumping can be distinguished according to whether or not the material has travelled. These types will be called respectively "parautochthonous" and "allochthonous" slumping.

Two varieties of parautochthonous slumping can be distinguished:

(i) Paramictic slumping. This process, and the structures associated with it, have been discussed in the preceding section.

*Comparison of figs 27 and 28 (loc. cit.), the corresponding captions, and the relevant portions of pp. 1037 and 1039 shows that the captions to these figures have been transposed.

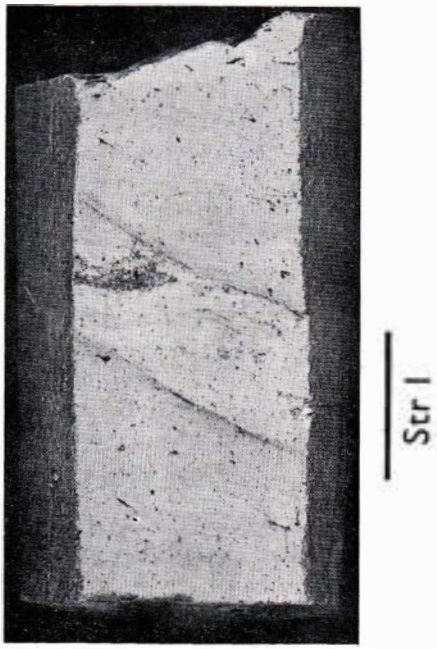

FIG. 23. Core E5, section Ph (photographed when dry). Two well-defined diagonal shear-planes are visible, separating a layer of very pale grey mud (Str 1) from pale sub-olive mud above and below. Remnants of bedding, lying approximately horizontal, are clearly visible in Str 1. (*Actual size*)

(ii) Shear plane slumping (fig. 23). This involves deformation by shear along discrete planes and apparently takes place in sediments which are stronger and more compacted than those in which paramixis occurs.

Shear plane slumping is found in core E5 from the central part of the slope. The numerous shear planes run diagonally across the core and can be seen truncating bedding in some places. Although E5 is a short core, and the shear planes extend to the surface, there can be little doubt that it was originally covered by at least several feet of sediment which have been stripped off by slumping or erosion. This is upheld by the fact that E5 is composed partly of grey mud, which extends to the top of the core; evidence from other cores indicates that the mud on the slope is always olive when first deposited, and only becomes grey after burial to a depth of several feet. The former presence of this overburden must have compacted and strengthened the sediment in E5 and this change in physical properties evidently caused the sediment to react to stress by shearing along discrete planes rather than by undergoing penetrative movement. The overburden was probably removed after the shear planes were formed, since there is no evidence (such as gashes in the sediment or the presence of foreign material) that the shear planes were formed near the sea bed.

Two types of allochthonous slumping can be distinguished in the present area:

(i) Creep-slumping, involving slow persistent movement of unconsolidated superficial sediment down a steep gradient (fig. 16).

(ii) Mudflows and sandflows, involving comparatively rapid movement of superficial sediment with sufficient momentum to carry the flow for a considerable distance across zones of low relief.

(i) Creep-slumping has been identified in two cores: A791, from the Wairarapa Arm, and A792, from the top of the slope near Cape Palliser. In both these cores, some type of slumping is evident from the presence of layers containing small dispersed pebbles. These pebbles are much larger than the average grain size of the ambient sediment and were evidently not transported by the currents which deposited the bulk of the material. Moreover, many of the pebbles in A792 are friable and stained brown with limonite. These brown pebbles, which have evidently suffered subaerial weathering, could not have been transported across the sea bed by currents without disintegrating. The transport of these friable pebbles can only be explained on the assumption that the matrix travelled downslope with the pebbles impelled by gravity. The lamination which occurs in parts of A791 and A792 probably represents bedding, sheared out by the creep-slumping process.

Even a rapidly moving slump might well have been sufficient to break up the friable pebbles and it is therefore probable that slumping took place relatively slowly. The name "creep-slumping" is accordingly suggested for this process. Although creep-slumping could not take place without the action of gravity, bioturbation of the superficial sediment may also play an important part in the process. The probability of bioturbation resulting in sediment creep on steep gradients has been mentioned by Emery (1953, fig. 3) with reference to observed benthic activity on a steep slope off southern California. Down-slope creep has also been observed in fossil sediments (Wood and Smith 1958, pp. 184–5).

The T-plane in A792 is probably caused by a sudden increase in the rate of creep-slumping, which might result from an abrupt steepening of the sea floor due to a vertical displacement along a submarine fault.

(ii) Mudflows and sandflows. A layer of sediment resulting from a mudflow occurs in A805, located near the centre of the Madden Depression. The uppermost layer in this core consists of unbedded mud with numerous pebble-size clasts some of which are angular fragments of soft mudstone; these clearly cannot have been transported over the sea bed by currents. The whole layer, including the mudstone fragments, probably originated near the head of the Madden Canyon and spread out as a thin sheet over the floor of the depression.

The muddy sand part of E7 apparently represents a sandflow. The presence of paramictic structure and the absence of bedding indicates that the sand was very rapidly deposited, possibly as a quicksand. The paramictic structure may in part be due to the expulsion of excess water

during stabilisation of the quicksand. The sandflow presumably originated as the result of unstable sand slumping in one of the nearby canyons. The most probable source of the sand is the Cook Strait Canyon. The tidal stream in the strait is constantly washing sand into suspension, and may well cause the deposition of unstable masses of sand in the upper reaches of the canyon system.

The hemipelagic mud at the top of E7 is evidently the product of slow, continuous deposition under normal conditions. The underlying "sandy layer with aggregates," however, probably represents the muddiest portion of the sandflow, the fine sediment having been concentrated near the top during deposition. At a later stage this layer was converted by burrowing organisms into a mass of muddy faecal pellets interspersed with small pockets of residual sand.

Slurried beds, resulting from sediment flow and probably involving considerable lateral displacement, have been described from both unconsolidated marine sediments and fossil sediments. These references include:

Ericson, Ewing, Heezen, and Wollin 1955 (plate 2, fig. 1): terrigenous sediment from the alluvial plain of the Hudson Canyon;

Ryan and Heezen 1965 (plate 4B): terrigenous sediments from the Ionian Sea;

Wood and Smith 1958 (plate VIII, fig. 4): Silurian greywackes and mudstones in Wales.

The various types of slumping found in the present area may be compared in general terms with the classification of subaqueous structures developed by Elliott (1965). Parautochthonous slumping would be "endokinematic" in Elliott's terminology (loc. cit., fig. 1) and would belong to the category of "horizontal transposition structures." Allochthonous slumping would also be "endokinematic," but would belong to the category of "translation slumps."

The "sediment behaviour" (Elliott, loc. cit.) is less easy to define. Paramictic slumping evidently corresponds to "corrugated bedding," "crumpled bedding," or "shredded bedding," while the mudflows and sandflows correspond to "slurried bedding." However, shear plane slumping as observed in the present area does not fit immediately into any of the sub-groups based on sediment behaviour; the mechanics of the process are obviously similar to those of "slide-bedding," but there is no evidence that in the present case the slumped masses have moved far from their original site of deposition. Again, creep-slumping does not fit easily into any of Elliott's categories, being intermediate between the "endokinematic" and "biokinematic" groups.

Relationship of Olive and Grey Types of Mud, and Evidence for Large-scale Slumping

A number of tests have been carried out in connection with the present work to determine the clay mineralogy of the two types of mud, and the reason for the colour difference. These experiments are now described.*

(1) Partial chemical analyses (Table 7) show that in some cases at least, there is no significant difference in total iron content or FeO/Fe_2O_3 ratio between olive and grey muds.

(2) X-ray diffractograms and infra-red absorption spectrograms show that there is no systematic difference in quality or quantity between the clay-size minerals in the olive and grey muds (Table 5).

(3) Heating separate samples of olive and grey mud to red heat in the presence of air turns both types a similar shade of pink.

(4) Overnight treatment of olive mud with 130-volume hydrogen peroxide containing a small proportion of nitric acid removes the olive hue, the sediment becoming very similar in colour to grey mud.

(5) Overnight treatment of olive mud with 3.7 percent sodium hypochlorite also removes the olive hue.

(6) Treatment of a moist surface sample of olive mud with acetone results in a pale yellow-green solution, although there is no colour change in the sediment. On the other hand, treatment of a moist surface sample of grey mud produces no coloration of the liquid.

(7) Determinations of amino acid content in samples of olive and grey muds (Table 8) show that these compounds are much more abundant and in much greater variety in olive mud than in grey.

The chemical analyses (1) show that the colour difference cannot be due to a difference in bulk iron content or in FeO/Fe_2O_3 ratio. It is also unlikely that the colours are due to differences in organic compounds within the clay mineral lattices, since the presence of interlayer organic compounds would produce a difference in layer spacing which would have been apparent on the X-ray diffractograms (2). The colours must therefore reside in the adsorbed layer on the surface of the clay particles.

The heating test (3) indicates that the colour difference between olive and grey must be connected in some way with adsorbed organic matter. All of the iron is presumably oxidised to the ferric state by the heating process and most of the organic matter will be removed by oxidation to carbon dioxide. A significant difference in adsorbed iron compounds would therefore have been revealed by a difference in intensity of the pink colouration, but this is not found. Any difference in adsorbed manganese

*With the exception of test (6), these tests were made on dried-out material. Test (6) was made on material containing original moisture, which had not dried out.

Table 7. Partial chemical analyses of selected core subsamples

Ferrous and ferric iron were determined by oxidation titration. FeO values could be high because of interference by organic matter.

Sample No.	$CaCo_3$%	*FeO%*	Fe_2O_3%
A795/MA1	4.5	2.5	1.4
A795/MA2	3.1	2.8 2.8	1.6 1.6
E8A/X1	10.2	2.9	1.7
E8A/X2	6.6	3.5	2.0
E9A/X1	22.6	2.2	1.7
E9A/X2	18.0	2.5	1.7
A807/MA1	4.6	3.0	1.6
A807/MA2	3.5	3.4	1.6
E2A/X1	3.6	3.1	1.7
E2A/X2	4.9	3.4	1.0
E13/X1	4.5	3.3 3.1	– 1.8
E13/X2	4.5	3.0 3.0	1.6 1.9
E2B/X1	3.3	3.0	1.5
E2B/X2	4.0	3.5	1.0

Table 8. Amino acid content (in μg/g) of samples of olive and grey mud

Amino acid	*E2A/X2 (olive)*	*E2B/X2 (grey)*
Leucine	21	14
Valine	19	10
Alanine	20	–
Threonine	–	–
Glycine	54	–
Serine	32	–
Glutamic acid	27	–
Aspartic acid	trace	–
Lysine	trace	–
Methionine	trace	–
Total	173	24

compounds would also have been revealed as a colour difference during the heating test.

The results of the hydrogen peroxide test (4) and the sodium hypochlorite test (5) clearly indicate that the colour of the olive mud is due to the presence of adsorbed organic compounds. Treatment with these reagents evidently destroys, by oxidation, the compounds responsible for the olive colour (and probably other organic compounds as well). Acidified hydrogen peroxide would remove adsorbed manganese compounds, but this possibility is eliminated by the sodium hypochlorite test. 2-, 3-, or 4-valent manganese would be converted to dark brown manganese dioxide by sodium hypochlorite, but the olive mud shows no evidence of a brown hue after treatment with this reagent.

The acetone treatment (6) confirms that freshly deposited olive mud contains olive-hued organic pigments in small quantities. However, the lack of colour change in the sediment sample indicates that if the colour is due to organic pigments, they are firmly bonded to the clay particles. These olive pigments probably include degradation products of chlorophyll: a number of such compounds are known, but for convenience these will be grouped together as "pheophytin" (cf. Orr, Emery, and Grady 1958).

If the above deductions are correct, it is clear that olive mud could change into grey mud as a result of organic diagenesis involving decomposition of the olive pigments. Independent evidence is provided by the relative abundance of amino acids in the olive and grey muds (7) which indicates that the grey mud has indeed suffered a greater degree of organic diagenesis than the olive mud. A progressive loss of amino acids from sediments with depth, presumably as a result of organic diagenesis, has been clearly demonstrated by Rittenberg *et al.* (1963, figs. 7, 8, and 9).

These deductions further imply that under conditions of steady continuous deposition, there should be a downward transition from olive mud into grey mud. Under less regular conditions, variations in colour might occur because of changes in the quality or quantity of clay particles or olive pigment supplied to the area, while interruptions in the olive-over-grey transition might result from local erosion or slumping. In spite of this, there should be a general downward change from olive to grey.

Among the several cores in the area which contain both olive and grey mud, only one (E13) shows a downward transition from olive to grey. It is evident that diagenesis is only one of a number of factors which determine the spatial relationships of the olive and grey mud. The relationships observed in cores other than E13 are now summarised and possible explanations suggested:

(a) Pale olive mud and pale sub-olive mud occur below grey mud in E4d and E5 respectively and interbanding of olive and grey occurs in sections of A795, A797, A807, A809, and A810.

Relationships of this kind might arise during slumping as a result of distortion or inversion of pre-existing olive-over-grey transitions. The same results, in terms of colour, could also be produced by variations in the supply rates of clay particles and olive pigment during sedimentation. Slumping is considered here to be the more likely alternative in E4d, E5, A807, and A810 since shear-plane slumping can be observed in E5 and all four of these cores occur in localities with relatively steep gradients where slumping would be expected. A795 and A809, however, occur in localities with relatively gentle gradients and in these cases the olive-to-grey variations are probably due to changes in the factors controlling sedimentation. The latter explanation probably also applies to A797; the gradient is steeper than at A795 and A809, but A797 shows well developed banding and lamination with no evidence of slumping.

(b) Abrupt upward increases in olive chroma occur at the T-planes in A795, A807, and A809.

The colour change in A795 is apparently connected with a sudden change in the sedimentary regime, and probably represents a reduction in the supply of clay particles relative to olive pigment. This is consistent with the suggestion that the T-plane in A795 corresponds to a sudden reduction in the supply of muddy detritus (see p. 26).

The colour changes at the T-planes in A809 can both be explained in terms of the erosion of an upper layer of sediment containing the olive-over-grey transition followed by the deposition of sediment with a higher proportion of olive pigment. This is likewise consistent with the suggestion that these T-planes are disconformities (see pp. 28–9). A similar explanation can be applied to the T-plane in A807, except that in this case the layer containing the transition was apparently removed by slumping (see p. 29).

(c) Grey mud extends to the top of four cores, two from the open slope (E4d and E5), and two from the Pahaua Canyon (E2b and E11). It cannot be supposed that no olive pigment is available at these localities, since they are all close to other localities where the cores consist partly or wholly of olive mud. The lack of olive mud at the tops of E4d, E5, E2b, and E11 therefore indicates that they represent areas of present-day non-deposition. This in turn implies that the average current velocity at these localities is slightly greater than in the immediate neighbourhood. A slight local increase in current velocity is readily explained on the assumption of a minor convexity on the sea bed. Such a convexity, however, cannot always have been present, for the grey mud in these cores must represent a comparatively recent depositional phase.

The simplest explanation appears to be that slumping of large masses of sediment has occurred on the slope and in the Pahaua Canyon. These masses of sediment may cover several square miles and may extend vertically downward for several tens of feet. Near the toe of such a slump material would be piled up and form a significant convexity on the sea floor. On the upper part of the convexity the bottom current velocity would be increased. If the superficial layer of olive mud was stripped off by slumping or erosion, the underlying grey mud would be exposed and would remain so if currents prevented further sedimentation.

Mechanical Properties of Olive and Grey Muds, and Their Relationship to the Possibility of Rhythmic Slumping

When the two types of mud are sedimented with sea water in a centrifuge, the compacted olive type has more interstitial water than the grey type, but the compacted grey mud is slightly weaker mechanically than the olive.

It is clear from these experiments that intergranular friction is significantly greater in the olive mud than in the grey variety. This relationship would explain the greater resistance of the olive mud to external shearing stress and would also explain the relative lack of compaction in the olive mud during sedimentation, since the process of compaction involves the sliding of clay particles over one another. The greater friction in the olive mud is presumably the result of the particular type of adsorbed layer covering the clay particles. Any compounds tending to neutralise the electrical charges on clay particles, or tending to bind particles together, have the effect of flocculating suspended clay or of increasing the friction between clay particles in more compacted material. The details of this process cannot yet be determined, since the components of the adsorbed layer have not been positively identified.

Whatever the basic reason for the difference in mechanical properties between the two types of mud, there can be little doubt that the olive mud passes downwards into relatively weaker grey mud. Diagenesis will not only cause the mud to become intrinsically weaker, but will also cause a rise in the interstitial water pressure, since less of the gravitational pressure in the mud is born by the mutual friction of clay particles. As a result the strength envelope will rise less steeply than with a chemically uniform sediment. The curve might even assume a negative gradient through a limited depth of sediment (compare figs 24 and 25).

Theory indicates that with muddy sediments deposited at a uniform rate on a uniform gradient periodic slumping with a well developed modal frequency would be expected. Given a firm substratum, sediment would accumulate until the shearing strength along a plane just above the substratum was exceeded by the downslope component of the vertical pressure, the latter being directly related to the sediment thickness. This situation is represented by the intersection of the strength envelope and stress locus (figs 24, 25). Slumping would then occur along a plane coinciding with, or just above, the substratum. Following the slump the accumulation of sediment would recommence, and continue until the appropriate thickness had again been deposited.

Given perfectly regular conditions, regular slumping would occur, but in practice the gradient of the sea bed varies from place to place (causing variations in the stress locus) and the rate of deposition varies with both time and place (causing variations in the strength envelope). Different parts of the sea bed therefore slump at different frequencies, and are usually out of phase with one another. Earthquakes also cause slumping to be more sporadic than would otherwise be the case, since the accelerations they impart give rise to externally imposed variations in the forces acting on the sediment: the point representing shearing stress and direct stress would no longer

lie on the static stress locus. Slumping thus is local, and very irregular when taken on a broad scale. If a narrow sector is considered, however, slumping within that sector shows a tendency towards regularity since the smaller the area the more uniform is the gradient and the rate of sedimentation.

The effect on slumping of changes in gradient and rate of sedimentation, and the effect of seismic forces, may be represented by converting the strength envelope and the stress locus into bands (figs 26 and 27) corresponding in width to the maximum probable range of variation of these parameters. Slumping could then occur under conditions represented by any point within the area where the two bands overlap. It can be shown that the most irregular slumping occurs when these bands intersect at an acute angle (fig. 26). Much greater regularity would be found if the two bands intersected at a wide angle (fig. 27). This condition may be fulfilled in the present area by the transformation of olive mud into grey mud.

FIGS 24–27

These diagrams all show the strength envelope and the stress locus for soft but cohesive sediments, deposited on a firm substratum which is not involved in slumping. It is assumed (i) that the upper surface of the sediment (the sea bed) is approximately parallel to its lower surface (the top of the firm substratum), and (ii) that the thickness of the sediment is small compared with its lateral extent. Under these conditions, any shear planes associated with slumping will tend to run parallel to the sediment layer. (Taylor, 1948, p. 418.)

The stress locus and strength envelope represent conditions along potential shear planes in the sediment. The "shear stress" and "direct stress" are components of the vertical pressure due to the sediment overlying a potential shear plane. If this pressure is denoted by P_v, its magnitude is given by $P_v = h \rho \cos \theta$, where h is the vertical thickness of the overburden, ρ is the mean submerged density of the sediment, and θ is the slope of the sediment layer. P_v may be resolved into two components: the shear stress (τ) directed downslope and given by $\tau = P_v \sin \theta$; and the direct stress (σ) normal to the slope and given by $\sigma = P_v \cos \theta$.

P_v will be equal to the submerged weight of accumulated sediment overlying unit area of the shear plane. This quantity will also be directly related to the sediment thickness, but since the density of the sediment varies due to compaction, the relationship will not be linear.

It is convenient here to represent the strength envelope as a relationship between shear strength and direct stress, although it has also been represented as a relationship between shear strength and vertical pressure, or between shear strength and overburden thickness.

The form and relationship of the strength envelope and the stress locus depend on the nature of the sediment and the conditions of deposition. Figs 24–27 show four possible situations:

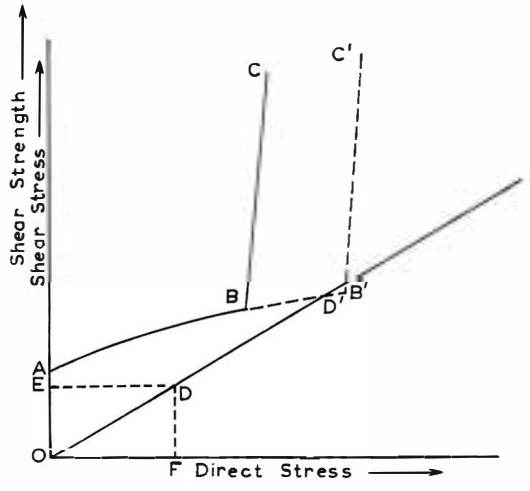

FIG. 24. The sediment is chemically uniform, and there are no variations in rate of deposition, variations in gradient, or earthquakes (this figure is adapted from Moore, 1961, fig. 3).

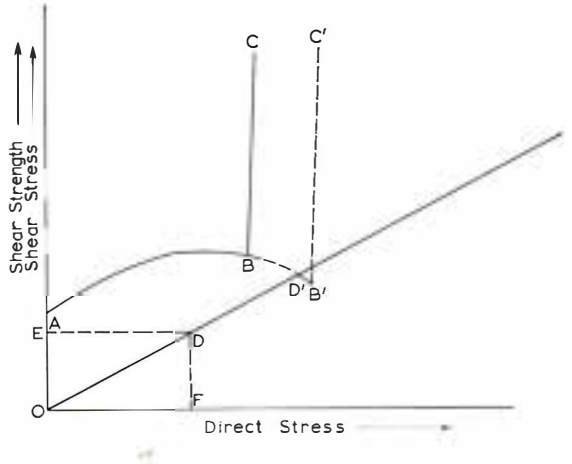

FIG. 25. The sediment is weakened in depth by chemical diagenesis, but there are no variations in rate of deposition, variations in gradient, or earthquakes.

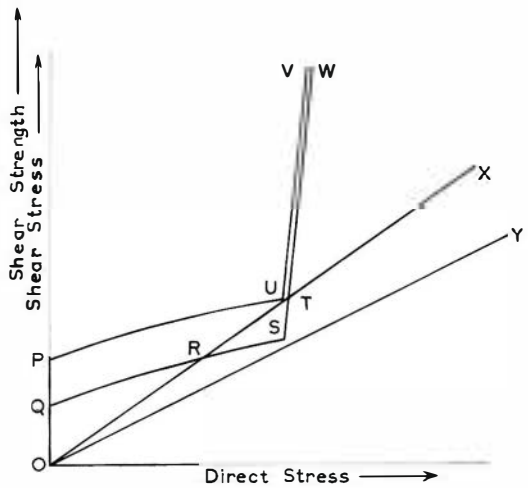

FIG. 26. The sediment is chemically uniform, but the strength envelope is affected by variations in rate of deposition, while the stress locus is affected by variations in gradient, and by variations in stress due to earthquakes. The effect of these variations may be represented by converting the strength envelope and the stress locus into bands corresponding in width to the maximum probable range of variation of these parameters.

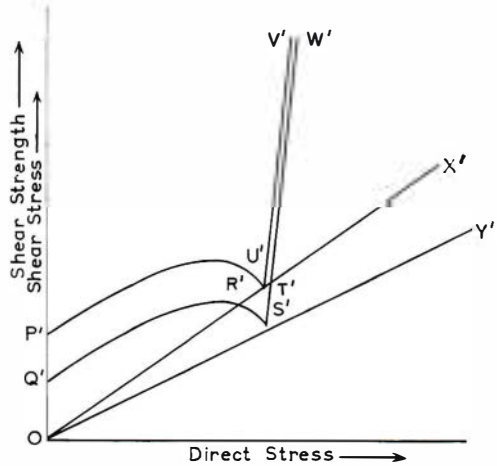

FIG. 27. The sediment is weakened in depth by chemical diagenesis, and affected by the same variations as the sediment represented in fig. 26.

LEGEND

In figs 24 and 25, ABC is the strength envelope, the portion AB representing the soft sediments, and the portion BC the substratum. The progressive accumulation of sediment would prolong the portion of the envelope representing the soft sediments, and would displace the portion representing the substratum away from the origin. ABC would become AB′C′.

ODD′ represents the stress locus, giving the relationship between the shearing stress and the direct stress. The angle DOF is the same as θ, the inclination of the slope. Point D corresponds to a plane in the sediment along which P_v = OD, τ = FD, and σ = ED.

In fig. 26, the area PQSU represents the portion of the strength envelope corresponding to the soft sediment, while SWVU represents the portion corresponding to the substratum. The area OXY represents the stress locus. The equivalent areas in fig. 27 are labelled P′Q′S′U′, S′W′V′U′, and OX′Y′.

The condition for instability is that the shearing stress must exceed the shearing strength. The onset of slumping may be illustrated by reference to figs 24 and 25. The envelope ABC, which lies entirely above the stress locus, represents a situation in which the accumulated thickness of sediment is not sufficient to cause slumping. As further sediment accumulates, however, the envelope moves progressively towards the position AB′C′; slumping can occur as soon as the envelope touches the stress locus at D′, although it may extend as far as AB′C′ if a small degree of metastability is allowed.

Under the conditions represented by fig. 26, slumping may occur at any point in the area RST. OT and OR represent vertical pressures, and the time intervals corresponding to OT and OR will be given by the formulae $I_t = OT/M_t$ and $I_r = OR/M_r$, where I_t and I_r are the time intervals, and the respective rates of sedimentation are M_t and M_r. Assuming that the greater the sedimentation rate the lower the intrinsic strength, M_r must be greater than M_t. I_t must therefore be greater than I_r (since OT is greater than OR). The ratio I_t/I_r is the ratio between the longest and shortest slumping interval in the area.

Under the conditions represented by fig. 27, slumping may occur at any point in the area R′S′T′. The ratio between the longest and shortest slumping intervals in the area ($I_{t'}$ and $I_{r'}$ respectively) will be given by the formula $I_{t'}/I_{r'} = OT'/OR' \times M_{r'}/M_{t'}$, where $M_{r'}$ and $M_{t'}$ are the rates of sedimentation corresponding to R′ and T′.

By inspection, OT′/OR′ is clearly smaller than OT/OR (fig. 26). Assuming that $M_{r'}/M_{t'}$ is of the same order of magnitude as M_r/M_t (fig. 26), $I_{t'}/I_{r'}$ will therefore be smaller than I_t/I_r. That is, slumping will be more regular in the system shown in fig. 27 than in the system shown in fig. 26.

CLASSIFICATION OF ORGANIC STRUCTURES

The organic structures may be classified as follows:

Individual structures	*Collective structures*
Sandy infilled burrows	Pseudolamination
Sandy relict burrows	Mottling
Aureole burrows	
Muddy burrows	
Meniscus burrows	
Faecal pellets	
Pale alteration burrows	
Miomelanosis	

Sandy Infilled Burrows (figs 17, 28, 29)

These take the form of cylindroid structures of sediment with a higher proportion of sand than the matrix. The central sandy zone may or may not be surrounded by an outer muddy zone, but in either case the sandy zone shows a relatively sharp outer boundary. The diameter of the sandy zone does not usually exceed 1 cm, although a few examples of up to 3 cm are found. This type of structure was evidently formed by sandy sediment filling up empty organic burrows with comparatively rigid walls.

The animals originally occupying the burrows would in some cases have moved elsewhere and others must have died and decomposed. The structures with a muddy outer zone apparently correspond to burrows made by species which select and bind muddy sediment to make a protective wall to the burrow. The grain size of sediment being deposited at any given time varies, being sometimes coarser or finer than the average sediment as a whole. During sandy phases, empty burrows would be filled up with sandy sediment and during muddy phases the burrows would be filled up with muddy sediment. In the latter case, whether a muddy wall was originally present or not, the result would be simply a muddy cylindroid structure. This is one type of "muddy burrow".

Empty burrows may be more likely to be filled in by sand than by mud. This would occur if the animals concerned showed a tendency to move or be killed during an influx of sand but were not disturbed by an influx of mud. This possibility, however, cannot be evaluated without knowing the habits of the organisms.

The decrease in abundance of these structures from the shelf to the ocean basin (Table 9) reflects a progressive decrease in the proportion of time occupied by sandy phases of sedimentation.

Descriptions and figures of sandy infilled burrows in unconsolidated marine sediments are moderately common in the literature. References to burrows of this type include:

Allen 1965 (plate 4D): sediments from the Niger Delta;

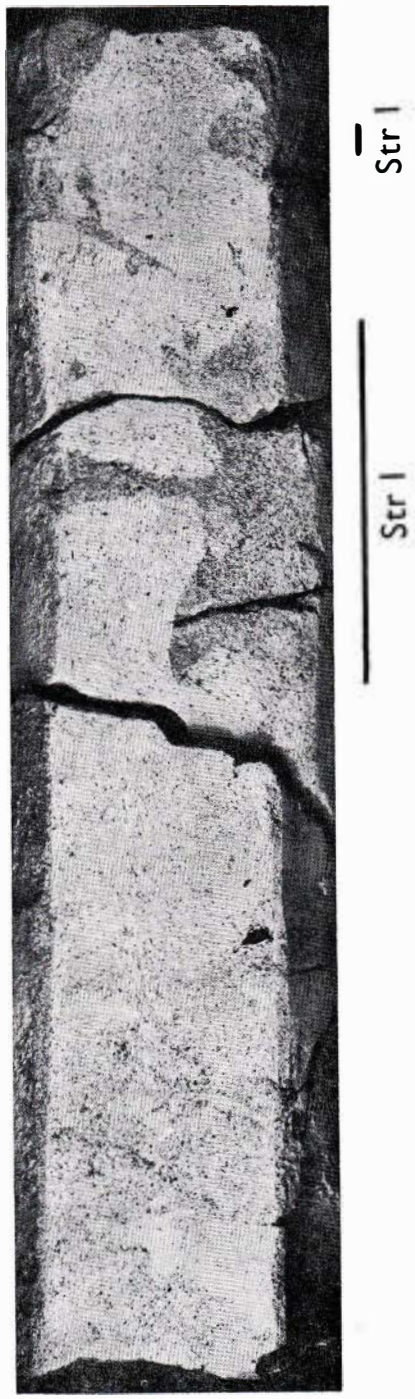

FIG. 28. Core A809, section Ph (photographed when dry). An example of sandy burrows without muddy walls (Str 1). The burrows are filled with pale olive very sandy mud, while the matrix consists of pale grey moderately sandy mud. (*Actual size*)

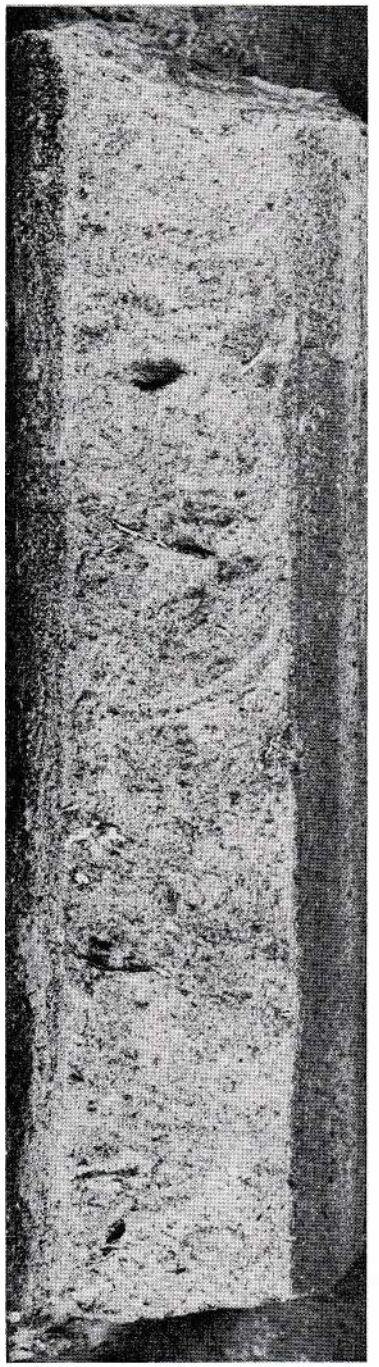

FIG. 29. Core A796, section Ph2 (photographed when dry). Pale olive very muddy sand, showing a longitudinal section of a sandy infilled burrow with muddy walls (Str 1). (*Actual size*)

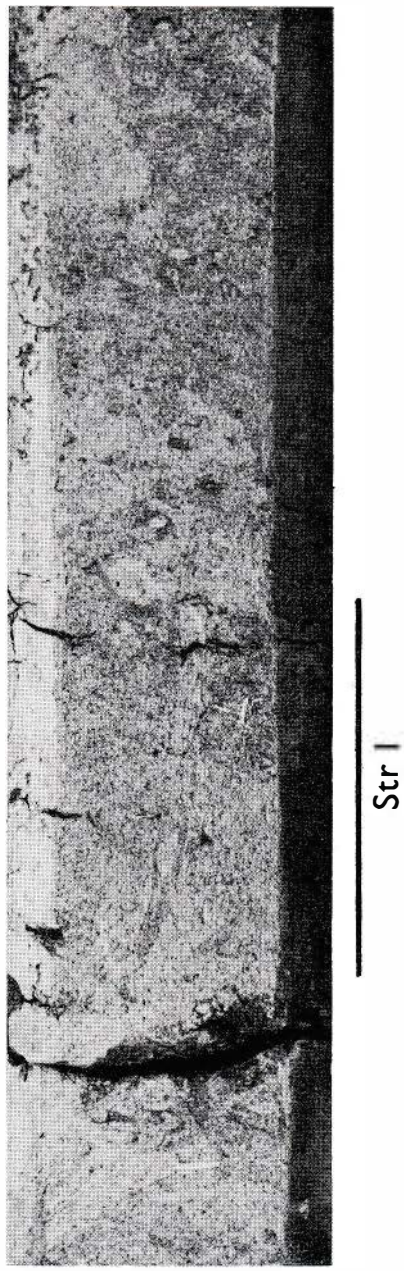

FIG. 30. Core A795, section Ph1 (photographed when dry). Pale olive very sandy mud, showing a longitudinal section of a near-vertical sandy relict burrow (Str 1), with muddy faecal material in the centre. (*Actual size*)

Bouma 1964 (fig. 19, upper part): terrigenous sediment from a canyon off California (the sandy burrows have muddy outer zones);

Greenman and LeBlanc 1965 (fig. 3, core 492, 5′ 3″–6′ 3″): terrigenous shelf sediments from the north-west Gulf of Mexico;

Moore and Scruton 1957 (fig. 10): terrigenous sediments from the shelf off central Texas;

Pantin 1960 (fig. 1D and E): terrigenous shelf sediments from Cook Strait, New Zealand;

Pantin 1966 (plate 2a, upper part): terrigenous sediments from the shelf in Hawke Bay, New Zealand;

Shepard and Einsele 1962 (plate III, figs 2 and 6): terrigenous sediments from a trough (San Diego) off California;

Table 9. Relative abundance of types of organic and inorganic structures and changes in abundance with bathymetric zone

Type of structure	*Shelf*	*Upper slope and canyons*	*Lower slope and trench*		*Ocean basin*
Inorganic					
Banding*	R	R	C (muddy sediments)	C (silty turbidites)	R
Lamination	R	M	N	C	R
T-planes	R	R (slope) N (canyons)	N	N	N
Convective paramictic structures	N	N	C	C	N
Slump structures	N	M	M	M	N
Organic (individual)					
Sandy infilled burrows	C	M	R	N	N
Sandy relict burrows	C	M	N	N	N
Aureole burrows	R	C	R	N	N
Muddy burrows	C	M	M	R	R
Meniscus burrows	C	M	R	N	N
Faecal pellets	M	C	R	N	R
Pale alteration burrows	N	N	M	N	C
Organic (collective)					
Pseudolamination	M	M	M	N	C
Grain-size mottling (muddy sediments)	C	C	C	—	C
Grain-size mottling (sandy sediments)	M	N	—	N	N
Colour mottling	N	N	R	N	M

*Conspicuous banding only is considered here

C = Common
M = Moderately common
R = Rare
N = Not found

van Straaten 1959 (figs. 7, 8, 10, 11): sediments from the Rhône Delta.

SANDY RELICT BURROWS (figs 12, 17, 30)

These are somewhat irregular ovoid or cylindroid structures, often with diffuse boundaries, of material more sandy than the matrix. They range up to about 1 cm in width. Their mechanical composition and diameter are more variable than that of sandy infilled burrows. These relict burrows evidently resulted from the passage of burrowing animals which ingested the finer fractions of sediment as they moved along. These fractions would have passed through the gut of each animal, the nutrients being extracted.

The fine material removed from the sediment during feeding must therefore be excreted by the animal and is, in many cases, in the form of faecal pellets, although the production of these pellets may not be continuous and may not occur in the same place as the original ingestion of the fine sediment. Some of these animals probably ascend to the sea bed before defaecation, while others defaecate sporadically within the sandy relict burrows. In other cases the ingestion of mud and the production of faecal material proceed continuously and more or less simultaneously; this results in the formation of aureole burrows.

Descriptions or figures of sandy relict burrows in unconsolidated marine sediments are comparatively rare in the literature. References to identifiable or possible sandy relict burrows include:

Bouma 1964 (fig. 19, central part): terrigenous sediments from a canyon off California;

Bouma 1965 (fig. 14, upper part): terrigenous sediments from a canyon off Baja California;

Pantin 1965 (plate 11B): sandy silt from a New Zealand fiord;

Rhoads and Stanley 1965 (fig. 2, core 3): intertidal sediments from a harbour in Massachusetts, U.S.A.

AUREOLE BURROWS (fig. 31)

These are twisting cylindroid structures with a sharply defined muddy core and a coarser outer zone with a relatively diffuse external margin. They range up to about 5 mm in width. The burrows are typically uniform in size and often occur in profusion. Strictly speaking they are a category of sandy relict burrows, but their distinctive nature justifies a separate term. In cross section the muddy core appears as a dark centre and is surrounded by a light-coloured aureole representing the coarser outer zone. The intimate relationship of the aureole and the inner zone shows clearly that they have been formed more or less simultaneously. This is the result of the ingestion of fine sediment from the outer zone and its excretion in the centre of the coarser material left by the slightly earlier passage of the animal.

Numerous ring-shaped structures in unconsolidated marine sediments have been described in the literature. Some of these are evidently mechanically differentiated structures, but others appear to be colour-differentiated structures with little mechanical difference between the inner and outer zones. Though the latter variety do possess "aureoles", the term "aureole burrows" will be reserved here for mechanically differentiated ring-shaped structures.

In published figures it is frequently very difficult to distinguish between aureole burrows and other ring-shaped structures because of the lack of detail in captions and text.

References to identifiable or possible aureole burrows include:

Arrhenius, 1952 (sections 2.45.6, 2.51.6, and 2.57.6; plate 2.6.2, core 51; plate 2.6.3, core 57): "eye-structures" in pelagic sediments from the east Pacific Ocean;

Ewing, Ericson, and Heezen 1958 (fig. 26, core A 185–35, 399–404 cm and 603–605 cm; same figure, core V3–107, 796–805 cm): sediments from the abyssal plain in the Gulf of Mexico, consisting of lutites interbedded with silty turbidites and a fine-grained calcareous turbidite.

Greenman and LeBlanc 1956 (fig. 5, core 536): lutite from the continental slope in the Gulf of Mexico;

Pantin 1966 (plate 2a, lower left): terrigenous sediments from the shelf in Hawke Bay, New Zealand;

Riedel and Funnell 1964 (numerous cores in plates 15, 17, 20–25, 27): "eye-structures" in pelagic sediments from the Pacific Ocean;

Shepard and Einsele 1962 (plate 11, fig. 3, centre): terrigenous sediments from a trough (San Diego) off California;

van Straaten 1959 (fig. 16): sediments from the Rhône Delta. Structures in the upper left corner of this figure have been interpreted by van Straaten (loc. cit., caption) as faecal pellets, but I consider that they are probably transverse sections of aureole burrows. Immediately to the right of these transverse sections, and also in the lower part of the same figure, occur structures which appear to be longitudinal sections of aureole burrows.

FIG. 31. Core A807, section Ph1 (photographed when dry). Pale olive mud, showing numerous aureole burrows. (*Actual size*)

MUDDY BURROWS (figs 17 and 32)

These can form in several ways which are not described here under separate headings, because the resulting structures are fairly uniform in texture and are very difficult to distinguish from one another.

The main types which theoretically could occur include muddy infilled burrows with a pre-existing muddy wall, muddy infilled burrows without such a wall, muddy relict burrows, and muddy faecal trails associated with the formation of sandy relict burrows elsewhere in the sediment. The cross-section of all the observed muddy burrows shows a circular or elliptical zone of sediment up to about 1 cm wide, which is significantly muddier than the surrounding matrix. In special cases the

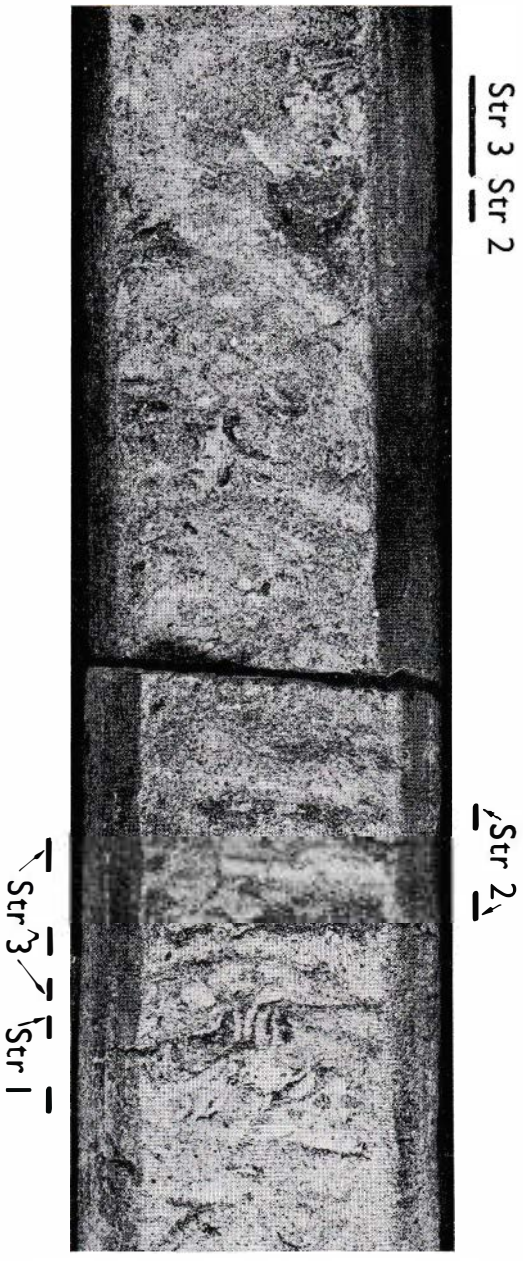

FIG. 32. Core A796, section Ph1 (photographed when dry). Pale olive very muddy sand, showing several types of organic structure: meniscus burrows (Str 1); sandy relict burrows (Str 2); and muddy burrows (Str 3). Pseudolamination is visible in the lower part of the core section. (*Actual size*)

origin of these burrows can be determined, but this is frequently impossible and the relative abundance of the various types is therefore problematical.

Descriptions and figures of muddy burrows in unconsolidated marine sediments are fairly common in the literature. References include:

Bouma 1964 (fig. 19, lower part, point 54): terrigenous sediment from a canyon off California;

Bouma 1965 (fig. 14): terrigenous sediment from a canyon off Baja California; swarms of small muddy burrows are visible in various parts of this figure;

Calvert and Veevers 1962 (fig. 4): lutite from the central Gulf of California;

Moore and Scruton 1957 (fig. 10): terrigenous sediments from the shelf off central Texas;

Pantin 1960 (fig. 1D, E, F): terrigenous shelf sediments from Cook Strait, New Zealand;

Pantin 1965 (plate 11B): sandy silt from a New Zealand fiord;

Pantin 1966 (plate 2a, lower right): terrigenous sediments from the shelf in Hawke Bay, New Zealand;

Riedel and Funnell 1964 (plate 14, core CAP 5 BP; plate 15, core Dolphin 2; plate 17, cores DWHH 27 and MSN 5 G; plate 21, core 143 P): dark burrows without "aureoles" in pelagic sediments from the Pacific Ocean;

Shepard and Einsele 1962 (plate 11, fig. 5, plate III, fig. 3): terrigenous sediments from a trough (San Diego) off California;

van Straaten 1959 (figs 14 and 15): sediments from the Rhône Delta.

MENISCUS BURROWS (figs 13, 22, and 32)

Meniscus structure may be found in burrows whose average mechanical composition is similar to that of the matrix, but may also occur in burrows which are either muddier or sandier than the surrounding sediment. The structure appears in section as a series of thin lunules with alternate lunules being relatively more muddy or sandy. In three dimensions these lunules must correspond to meniscus-shaped lamellae, roughly circular when viewed along their axis but crescent-shaped when viewed at right angles to the axis. Individual lamellae clearly represent soft faecal material packed into the tube occupied by the animal as it moved along. The animal apparently ingested sediment in bulk, but in the alimentary canal the coarse and fine components became fractionated. It seems likely that the muddy sediment would pass through the gut more readily than the sandy material and after each feeding period a new muddy lamella would be pushed out behind the animal followed by a sandy lamella.

The occurrence of meniscus burrows which differ in average grain-size from the matrix indicates either (i) that one particular size range (fine or coarse) was preferentially selected by the animal, or (ii) that the animal was defaecating in sediment with a slightly different mechanical composition from that in which it was feeding. In the first case, the matrix surrounding the burrow would be enriched in the rejected size range. This zone of enrichment is rarely seen, indicating that the second process is more common.

Meniscus burrows are very distinctive, and have been reported from both unconsolidated marine sediments and fossil sediments. References to these burrows include:

Arrhenius 1952 (section 2.40.6; plate 2.6.1, core 39, burrows located at 57 cm, 287 cm, 495 cm, and 506 cm; plate 2.6.7, core 40, several burrows between 872 and 884 cm): pelagic sediments from the east Pacific Ocean;

Bouma 1964 (fig. 3, point 49; fig. 5, points 38 and 40; fig. 9, point 38): terrigenous sediments from a canyon off Baja California, and from the central Gulf of California;

Bouma 1965 (fig. 14, point 18): terrigenous sediments from a canyon off Baja California;

Greenman and LeBlanc 1956 (fig. 5, core 127, 2–4 in. from top of section): lutite from the continental slope in the Gulf of Mexico;

Kuenen 1961 (fig. 3): Cretaceous sandstone from Westphalia, Germany; this author uses the name "arched structures" for these burrows, but the term "meniscus burrows" is more descriptive;

Norris 1964 (fig. 13): phosphorite nodule from the Chatham Rise, New Zealand;

Pantin 1960 (fig. 1F): terrigenous shelf sediments from Cook Strait, New Zealand;

Riedel and Funnell 1964 (plate 23, core 151 P, burrows at 20 cm, 37 cm, 41 cm, and 60 cm): pelagic sediment from the Pacific Ocean;

Schaefer 1962 (pp. 348–50 and fig. 183): *Echinocardium* burrow in sandy sediments from the North Sea;

van Straaten 1959 (fig. 2, upper centre): terrigenous sediments from the Dutch Wadden Sea.

Faecal Pellets (fig. 11)

Muddy faecal pellets have been identified in muddy sediments from all the main bathymetric environments, although recognition is frequently difficult owing to the similar mechanical composition of pellets and matrix. The most conspicuous pellets of this type are found in the sandy layers with aggregates which occur in the Pahaua and Madden Canyons and at one locality (E7) in the Hikurangi Trench. In these layers there is an obvious difference between the pellets and the matrix.

Some of the pellets in the various sandy layers with aggregates have evidently been formed *in situ* while others have not. When lamination is present the pellets must represent material transported from elsewhere along with other sand-size particles. On the other hand, the pellets in the layer which occurs in E7 were apparently formed in place, since the layer in question is underlain by sand and there is no other visible source for the pellets.

The non-laminated sandy layers with aggregates (in cores other than E7) must include formerly laminated examples with transported pellets, but it is very unlikely that all the pellets in these non-laminated layers are transported. Many of the layers probably contain both transported and locally formed pellets, while other layers may contain only the locally formed variety.

The difference in texture between pellets and matrix in the sandy layers with aggregates would become progressively accentuated during pellet formation, because the pellet-forming animals selectively ingest the finer sediment fractions and must therefore leave the coarser material behind. The end result may be a mass of muddy pellets interspersed with relict pockets of sand as in E7.

Muddy faecal pellets are locally abundant in some unconsolidated marine sediments. References describing or figuring pellets of this type include:

Allen 1965 (plate 6F): sediments from the Niger Delta;

Arrhenius 1952 (section 2.39.6; plate 2.6.7, horizontal section of core 39 at 508 cm): pelagic sediments from the east Pacific Ocean;

Bouma 1964 (fig. 5, centre): terrigenous sediments from the Gulf of California; one of the clusters of faecal pellets corresponds to a meniscus burrow (point 40);

Pantin 1965 (plate 11B): sandy silt from a New Zealand fiord.

Pale Alteration Burrows (figs 9, 22, 33, and 34)

The hemipelagic and pelagic muds in the trench and the ocean basin contain a type of burrow whose identification depends not on differences in the grain size of the sediment but on differences in colour. These muds are typically pale olive, very pale olive, or pale sub-olive, but the colour shows considerable small-scale variation. In particular, there occur circular, elliptical, or parallel-sided patches which are significantly lighter in colour than the matrix. These patches range up to about 1 cm in width and tend to lie horizontally. They clearly represent sections of burrows with a circular or elliptical cross-section, and with a strong tendency to lie within a horizontal plane. When numerous these burrows may give rise to pseudolamination. They usually show no internal variation, although faint meniscus structure is occasionally seen.

In spite of the colour difference there is usually no significant difference in grain size between the burrows and the matrix, indicating that the burrows represent faecal trails formed by animals which ingest the sediment in bulk but cause little or no grain-size fractionation in the gut. There can also be little or no compaction of the sediment in the gut, since there is no evidence of pelleting.

The burrows are typically lighter in colour than any part of the matrix in the immediate vicinity.

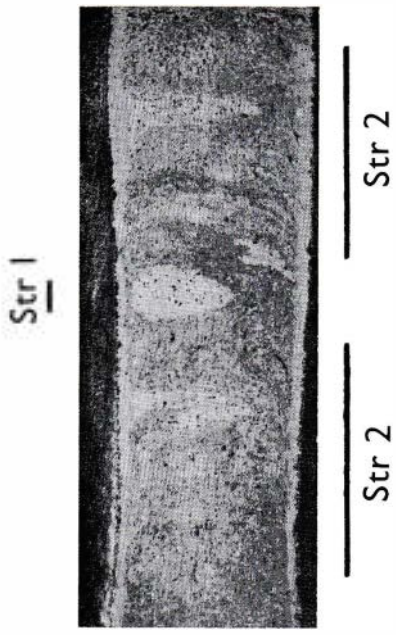

FIG. 33. Core E9A, section Ph2 (photographed when dry). Pale to very pale sub-olive mud, with numerous forams: this part of the core contains a well-marked pale alteration burrow (Str 1) and colour mottling (Str 2). (*Actual size*)

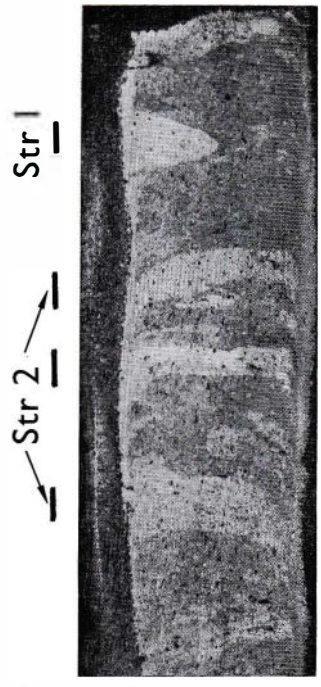

FIG. 34. Core E9A, section Ph1 (photographed when dry). Pale to very pale sub-olive mud with numerous forams. A pale alteration burrow is seen in cross-section (Str 1); several longitudinal sections of similar burrows (Str 2) give rise to pseudolamination. (*Actual size*)

Thus the burrows cannot be explained as infillings derived from other parts of the sediment in which the colour was different. It therefore appears that although there has been virtually no mechanical alteration of the sediment in the burrows, chemical alteration accompanied by a colour change has taken place.

The following experiments have been carried out to determine the nature of this chemical alteration.*

(1) Overnight treatment of samples from burrows and matrix with 130-volume hydrogen peroxide, containing a small proportion of nitric acid, removes the olive hue from both types of material converting both to the same shade of light grey. Overnight treatment with 3.7 percent sodium hypochlorite gives a similar result.

(2) Treatment of samples from burrows and matrix with hydrochloric acid (to remove the calcium carbonate) causes both types of material to become considerably darker than equivalent samples immersed in water, but the difference between burrows and matrix is removed.

(3) Heating a sample containing a pale alteration burrow to red heat in the presence of air causes both burrow and matrix to turn pink, but the burrow turns a lighter shade of pink than the matrix.

(4) X-ray diffractograms and infra-red absorption spectrograms indicate that there is no essential difference in quality or quantity between the clay-size minerals in the burrows and the surrounding matrix (E8A/X1–2 and E9A/X 1–2 in table 5).

The hydrogen peroxide and sodium hypochlorite tests (1) indicate that the olive chroma of both matrix and burrows is due to adsorbed organic matter, and that the matrix contains more of this than the burrows. However, treatment with hydrochloric acid (2) shows that the difference in lightness between burrows and matrix probably resides in the quantity of organic matter adsorbed on to calcilutite particles. This difference would be expected to persist even after the removal of the carbonate fraction, if it was due to the quantity of organic matter associated with non-calcareous clay-size minerals.

The similarity of the clay-size minerals in burrows and matrix (4) shows that the difference in lightness cannot be due to bulk differences in the mineralogy of the clay-size particles.

The heating test (3) indicates that the clay particles in the burrows carry a lower concentration of adsorbed iron compounds than clay particles in the matrix. This difference does not seem, however, to exercise a fundamental influence on the colour of either type of sediment.

*These tests were carried out on dried-out material.

Adsorbed organic matter has evidently been removed from the calcilutite in the burrow sediment as a result of chemical processes associated with the ingestion and excretion of the sediment by animals. This phenomenon is probably due to the vigorous bacterial activity which would be expected in sediment passing through the gut of an animal and in the corresponding faecal material. Although the organic content of the faecal material would at first be much higher than that of the matrix, the high bacterial population might result in the removal of not only most of the free organic matter but some of the adsorbed organic matter as well.

Chemical reactions associated with ingestion and excretion of sediment have apparently also caused the removal of adsorbed iron from clay particles. Reduction of adsorbed iron might occur as a result of contact with organic matter, with bacteria playing some part, possibly a fundamental part, in the process of reduction. If most of the adsorbed iron was reduced to the ferrous condition, it would probably be lost rapidly. Sea water contains virtually no ferrous iron and consequently ferrous ions at the surface of the clay minerals would show a strong tendency to diffuse away in solution. These ions might later be re-oxidised and re-adsorbed on to clay particles but if this occurred, the adsorbed iron would be distributed through the sediment rather than concentrated in those parts where it originated; that is, the clay particles in the burrows. Some of the ferrous ions might even reach the sea water overlying the sediment, where they would be re-oxidised to colloidal ferric compounds (hydroxide and possibly phosphate) and removed by diffusion and turbulence. The overall effect of these processes would be the removal of adsorbed iron from the burrows.

Structures resembling in appearance the "pale alteration burrows" of the present area seem to be widespread in unconsolidated deep-sea sediments, although there is no proof that these structures were all formed by the same mechanism. Examples of structures from other areas resembling the "pale alteration burrows" can be found in the following references:

Arrhenius 1952 (plate 2.6.1, core 39; plate 2.6.2, cores 42, 51 and 54; plate 2.6.4, core 58; plate 2.6.8, core 45; plate 2.6.9, core 58): pelagic sediments from the east Pacific Ocean; this author gives a possible mechanism for the development of these particular structures (loc. cit., section 1.12.6);

Calvert and Veevers 1962 (fig. 6): pelagic sediment from the experimental Mohole;

Riedel and Funnell 1964 (plate 14, core CK 16; plate 15, core DWBG 5; plate 16, core DWHH 13; plate 17, core DWHH 34; plate 18, core MSN 10 G; plate 20, MSN 142 G; plate 23, MSN 153 PG; plate 26, TET 29): pelagic sediments from the east Pacific Ocean.

MIOMELANOSIS AND MIOMELANOTIC ZONES (figs 9, 22, and 35)

This rather striking phenomenon came to my notice in the following way. Core series E was collected in August 1963, sealed in iron barrels, and extruded some 2 weeks later. The cores were then securely wrapped with the partial exclusion of air, packed in cases, and dispatched by sea to the U.K. When the cases were opened in February 1964 many of the cores in series E were still damp and some contained a dark sulphide-bearing zone in the centre. Evidently the cores had become anaerobic through the rapid bacterial decomposition of organic matter while sealed up, but the sulphide had been partially re-oxidised by the slow diffusion of air.

When certain cores were opened it was found that the areas of dark sulphide were interrupted by lighter-coloured patches with little or no sulphide. Further examination showed that the sulphide-poor areas correspond to organic burrows. These burrows can be seen in the peripheral non-sulphide zone in the form of patches with a slightly lighter colour than the matrix. They are in fact pale alteration burrows.

The local sulphide-poor areas will be called "miomelanotic* zones," and the set of processes giving rise to them "miomelanosis."

Several explanations for miomelanosis can be suggested. For bacteria to produce iron sulphide in such an environment, there must be:

(i) adequate supply of iron compounds;
(ii) adequate supply of sulphur compounds;
(iii) sufficiently low redox potential;
(iv) adequate bacterial population.

Miomelanotic zones must be due to the absence of at least one of these four conditions. Two factors, however, can be ruled out with a fair degree of certainty. The sulphur in the black sulphide must be derived from dissolved sulphate in the interstitial sea water, and there is no reason to suppose that the concentration of sulphate was any less in the miomelanotic zones than elsewhere. Again, the redox potential in the miomelanotic zones must often have been sufficiently low for sulphide to form, since many of these zones appear to be completely surrounded by sulphide-bearing sediment. One must therefore suppose that either a sufficient supply of iron was not available, or else that the growth of anaerobic bacteria was somehow inhibited.

It has been suggested in the previous section that adsorbed iron may have been removed from the clay particles in the pale alteration burrows. If this is so, it may also be an explanation for miomelanosis. The bulk percentage of sulphide in the dark material is very small, and the iron it contains could easily be accounted for

*Derived from the Greek *mio* (less) and *melas* (black).

in terms of iron previously adsorbed on to clay particles. Assuming that adsorbed iron was essential for the development of iron sulphide the depletion or absence of this iron might well cause miomelanosis.

The second possibility, that the growth of anaerobic bacteria was prevented in the miomelanotic zones, is difficult to assess without microbiological work on fresh material from the same area. The inhibition of bacteria in the miomelanotic zones could be due to several causes, for instance:

(i) lack of proper nutrients;
(ii) antibiosis associated with the local growth of organisms which did not precipitate iron sulphide;
(iii) antibiosis due to residual non-living organic compounds;
(iv) the action of bacteriophages.

Any of these effects might arise from the special biochemical environment which must occur in organic burrows, an environment which presumably differs in many ways from that in the matrix. Until a considerable amount of microbiological work has been done on similar material it will not be certain which of these effects, if any, is the true explanation for miomelanosis.

PSEUDOLAMINATION (figs 32, 34, and 36)

This structure, which may closely resemble true lamination when seen on a flat surface, takes the form of numerous sub-horizontal sedimentary units up to a few millimetres thick. These units may be either slightly or strongly differentiated in terms of grain size. Detailed examination reveals that while true lamination also consists of sub-horizontal units, these units extend laterally in all directions and when a particular unit disappears it wedges out gradually. In pseudolamination the units are elongated or linear and disappear rather abruptly with the edge of a particular unit being frequently rounded. It is thus clear that pseudolamination, is due to large numbers of organic burrows produced by animals which wandered freely within a particular level but did not move upwards or downwards to any extent. Organisms such as the polychaete worm *Nereis* (Schaefer, 1962, pp. 328–9 and fig. 166) are known to behave in this way.

Individual burrows in a pseudolaminated sediment may belong to one or more of the varieties described in the preceding sections. Although the burrows causing pseudolamination in the present area do not exceed 1 cm in width, a similar structure composed of burrows over 1 cm in width (pseudobanding) is found in other areas.

Pseudolamination and pseudobanding are present in many unconsolidated marine sediments and may be more widespread than has

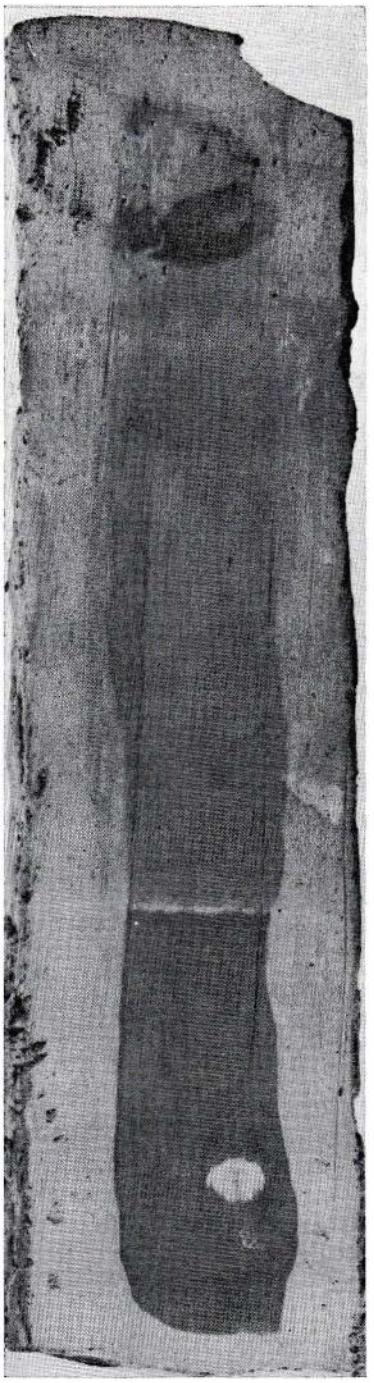

FIG. 35. Core E8A, section Ph1 (photographed when damp). Mud (pale to very pale olive when dry) with a dark sulphide-bearing zone in the centre and a well-marked pale alteration burrow (Str 1) showing miomelanosis. (*Actual size*)

FIG. 36. Core E11, section Ph (photographed when dry). Pale grey moderately sandy to very sandy mud, showing pseudolamination. The well-defined near-horizontal structure (Str 1) is evidently a longitudinal section of a sandy relict burrow, with muddy faecal material in the centre. This structure indicates the origin of the fainter pseudolamination above and below. (*Actual size*)

generally been recognised. References with examples of pseudolamination or pseudobanding include:

Arrhenius 1952 (plate 2.6.7, core 40; plate 2.6.2, core 51): pelagic sediments from the east Pacific Ocean;

Bouma 1965 (fig. 14): terrigenous sediment from a canyon off Baja California;

Riedel and Funnell 1964 (plate 22, core MSN 146 P; plate 23, core MSN 151 P; plate 24, cores MSN 153 P and MSN 154 P): pelagic sediments from the Pacific Ocean;

van Straaten 1959 (figs 14 and 16): sediments from the Rhône Delta.

MOTTLING (figs 11, 22, and 33)

This structure may be defined as an abundance of irregular patches of sediment, differentiated from one another and from the matrix by variations in grain size, colour, or both. Individual units may be either weakly or strongly differentiated and boundaries may be diffuse or well defined.

Mottling is evidently formed by the repeated disturbance of bottom sediments by crawling and burrowing organisms. In general, mottling may represent either disturbed organic burrows or disturbed bedding but in the present area disturbed burrows appear to be mainly responsible. In the following discussion "mottling" is reserved for situations in which even the organic burrows have been partially destroyed by incessant animal movement. The term is not used here for well defined burrows, even when abundant. "Grain-size mottling" is used for structures differentiated principally by variations in grain size (figs 11 and 22), while "colour mottling" is used for structures differentiated principally (or entirely) by colour variations (fig. 33).

Grain-size mottling is common in all the bathymetric environments, but is mainly confined to sediments which consist dominantly of mud. Moreover, the mottling is usually very indistinct through lack of differentiation between mottles and matrix. Dominantly sandy sediments with grain-size mottling are moderately common on the shelf but have not been observed in the other bathymetric environments. This dependence of the abundance of mottling on grain size is presumably due to the mechanical properties of the sediments involved, mud being more easily stirred than sand.

Colour mottling, resulting from the disturbance of pale alteration burrows, is moderately common in the ocean basin but is often indistinct because of relatively weak differentiation of the component colours. Moreover, colour mottling is noticeably less common in these sediments than grain-size mottling. This indicates that some of the pale alteration burrows are formed at a lower level in the sediment than the grain size mottling, in a zone where most of the mechanical disturbance has ceased.

Grain size mottling is common in unconsolidated marine sediments. References with descriptions or figures of this type of structure include:

Bouma 1964 (fig. 19): terrigenous sediment from a canyon off California;

Bouma 1965 (fig. 14): terrigenous sediment from a canyon off Baja California;

Ericson, Ewing, and Wollin 1963 (fig. 2, cores V3–153, V3–152, and V3–151): pelagic sediments from the western part of the North Atlantic Ocean;

Greenman and LeBlanc 1956 (fig. 5, cores 127 and 345): lutites from the continental slope in the Gulf of Mexico;

Moore and Scruton 1957 (figs 5, 7, 10): terrigenous sediments from the shelf off central Texas;

Pantin 1966 (plates 2c and 3c): terrigenous sediments from the shelf in Hawke Bay, New Zealand;

Shepard 1956 (plate VII, fig. 3): sediment from the Mississippi Delta;

Shepard 1958 (figs 2A and 7): terrigenous sediments from coastal waters off central Texas.

Colour mottling is also widespread, but appears to occur mainly in deep-sea sediments. References with descriptions or figures of this type of mottling include:

Arrhenius 1952 (plate 2.6.1, core 39; plate 2.6.2, cores 42 and 51): pelagic sediments from the east Pacific Ocean;

Ericson, Ewing, and Wollin 1963 (fig. 2, cores V15–164, V16–21, and V12–5): pelagic sediments from the Atlantic Ocean;

Greenman and LeBlanc 1956 (fig. 6, core 339): lutite from the abyssal plain in the Gulf of Mexico;

Riedel and Funnell 1964 (numerous cores on plates 14–8 and 20–7): pelagic sediments from the Pacific Ocean.

RELATIVE ABUNDANCE OF INTERNAL STRUCTURES

Even in a single core, considerable variations in the relative abundance of different types of structure often occur. In spite of this variability, however, the overall abundance of internal structures can be estimated qualitatively by considering the whole series of cores (Table 9).

A conspicuous feature of the variations in abundance, on both a broad and a local scale, is the well marked inverse correlation between the presence of lamination and of organic structures. All non-laminated sediments in the area have suffered bioturbation to a greater or lesser extent. It is highly probable that other less obvious correlations (either direct or inverse) will be found between structures of different types.

ACKNOWLEDGMENTS

Analyses for clay size minerals by infra-red absorption spectrometer were carried out by Mrs J. Montgomery (New Zealand Soil Bureau) and interpreted by Dr M. Fieldes (Director, New Zealand Soil Bureau); analyses for clay minerals by X-ray diffractometer were carried out by R. S. Freeman (New Zealand Geological Survey) and R. Bradshaw (Geology Department, Bristol University). Dr R. H. Clarke (then at the Geology Department, Bristol University) determined the amino acid content of the muds; chemical analyses of sediments were made by Chemistry Division, DSIR: I am grateful for the help given by these persons and institutions.

I thank the master and crew of m.v. *Taranui* for their willing help at sea; fellow members of the Institute staff who assisted with sampling operations; J. C. McDougall and the sediment laboratory staff for grade analyses, and Miss P. Lawrence for help in drawing diagrams.

I also wish to thank the Royal Society and Nuffield Foundation for the award of a Commonwealth Bursary to cover expenses at the Geology Department, Bristol University, where much of the work was done.

I must also express my indebtedness to the late Professor W. F. Whittard for providing facilities at Bristol, and to him and numerous other colleagues at Bristol and the New Zealand Oceanographic Institute for many interesting and informative discussions during the course of the work.

Photographs used in figs 9, 10, 18, 19, 22, and 35 were taken by Mr E. W. Seavill, Geology Department, Bristol University. The remainder were taken by Photographic Section, Information Service, DSIR.

REFERENCES

ALLEN, J. R. L. 1965: Late Quaternary Niger Delta, and adjacent areas: sedimentary environments and lithofacies. *Bull. Am. Ass. Petrol. Geol. 49*: 547–600.

ARRHENIUS, G. 1952: Sediment cores from the east Pacific. *Rep. Swed. deep Sea Exped. V, Parts 1–4. 227 pp., Append. Part 2.* pls 2.6.1–2.6.2.

BAGNOLD, R. A., 1956: The flow of cohesionless grains in fluids. *Phil. Trans. R. Soc. A 249*: 234–97.

——— 1963: Mechanics of marine sedimentation. *In* Hill, M. N. (Ed.) "The Sea. 3". John Wiley, New York.

BATES, C. C. 1953: Rational theory of delta formation. *Bull. Am. Ass. Petrol. Geol. 37*: 2119–62.

BOUMA, A. H. 1964: Notes on X-ray interpretation of marine sediments. *Mar. Geol. 2*: 278–309.

——— 1965: Sedimentary characteristics of samples collected from some submarine canyons. *Mar. Geol. 3*: 291–320.

BRODIE, J. W. and HATHERTON, T. 1958: The morphology of Kermadec and Hikurangi Trenches. *Deep Sea Res. 5*: 18–28.

CALVERT, S. E. and VEEVERS, J. J. 1962: Minor Structures of unconsolidated marine sediments revealed by X-radiography. *Sedimentology 1*: 287–95.

COLEMAN, J. M., GAGLIANO, S. M., and WEBB, J. E. 1964: Minor sedimentary structures in a prograding distributary. *Mar. Geol. 1*: 240–58.

DANGEARD, L., MIGNIOT, C., LARSONNEUR, C., and BAUDET, P., 1964: Figures et structures observées au cours du tassement des vases sous l'eau. *C. r. Acad. Sci. Paris 258*: 5935–8.

DAVIES, H. G. 1965: Convolute lamination and other structures from the Lower Coal Measures of Yorkshire. *Sedimentology 5*: 305–25.

ELLIOTT, R. E., 1965: A classification of subaqueous sedimentary structures based on rheological and kinematical parameters. *Sedimentology 5*: 193–205.

EMERY, K. O. 1953: Some surface features of marine sediments made by animals. *J. sedim. Petrol. 23*: 202–4.

ERICSON, D. B., EWING, M., HEEZEN, B. C., WOLLIN, G. 1955: Sediment deposition in deep Atlantic. *Spec. Pap. geol. Soc. Am. 62*: 205–20.

ERICSON, D. B., EWING, M., and WOLLIN, G. 1963: Pliocene-Pleistocene boundary in deep-sea sediments. *Science, N.Y. 139*: 727–37.

——— 1964: Sediment cores from the Arctic and Subarctic Seas. *Science, N.Y. 144*: 1183–92.

EWING, M., ERICSON, D. B., and HEEZEN, B. C. 1958: Sediments and topography of the Gulf of Mexico. *In* Weeks, L. G. (Ed.) "Habitat of Oil". American Association of Petroleum Geologists, Tulsa.

GEOLOGICAL SOCIETY OF AMERICA 1963: "Rock Colour Chart". Geological Society of America, New York.

GORSLINE, D. S. and EMERY, K .O. 1959: Turbidity-current deposits in San Pedro and Santa Monica basins off southern California. *Bull. geol. Soc. Am. 70*: 279–90.

GREENMAN, N. N. and LEBLANC, R. J. 1956: Recent marine sediments and environments of northwest Gulf of Mexico. *Bull. Am. Ass. Petrol. Geol. 40*: 813–47.

HULSEMANN, J. and EMERY, K. O. 1961: Stratification in Recent sediments of Santa Barbara Basin as controlled by organisms and water character. *J. Geol. 69*: 279–90.

KUENEN, PH. H. 1961: Some arched and spiral structures in sediments. *Geologie Mijnb. 40*: 71–4.

——— 1965: Value of experiments in geology. *Geologie Mijnb. 44*: 22–36.

MIDDLETON, G. V. 1966: Small-scale models of turbidity currents and the criteria for auto-suspension. *J. sedim. Petrol. 36*: 202–8.

MOORE, D. G. 1961: Submarine slumps. *J. sedim. Petrol. 31*: 343–57.

MOORE, D. G. and SCRUTON, P. C. 1957: Minor internal structures of some recent unconsolidated sediments. *Bull. Am. Ass. Petrol. Geol. 41*: 2723–51.

NORRIS, R. M. 1964: Sediments of Chatham Rise. *Bull. N.Z. Dep. scient. ind. Res. 159. (Mem. N.Z. Oceanogr. Inst. 26.)*

ORR, WILSON L., EMERY, K. O., and GRADY, J. R. 1958: Preservation of chlorophyll derivatives in sediments off southern California. *Bull. Am. Ass. Petrol. Geol. 42*: 925–62.

PANTIN, H. M. 1960: Dye-staining technique for examination of sedimentary microstructures in cores. *J. sedim. Petrol. 30*: 314–6.

——— 1963: Submarine morphology east of the North Island, New Zealand. *Bull. N.Z. Dep. scient. ind. Res. 149. (Mem. N.Z. Oceanogr. Inst. 14.)*

——— 1964: Sedimentation in Milford Sound. *In* Skerman, T. M. (Ed.) "Studies of a southern fiord." *Bull. N.Z. Dep. scient. ind. Res. 157. (Mem. N.Z. Oceanogr. Inst. 17.)*

——— 1966: Sedimentation in Hawke Bay. *Bull. N.Z. Dep. scient. ind. Res. 171. (Mem. N.Z. Oceanogr. Inst. 28.)*

——— 1969: The appearance and origin of colours in muddy marine sediments around New Zealand. *N.Z. Jl. Geol. Geophys 12*: 51–66.

PETTIJOHN, F. J. and POTTER, P. E. 1964: "Atlas and Glossary of Primary Sedimentary Structures". Springer-Verlag, New York.

RHOADS, D. C. and STANLEY, D. J. 1965: Biogenic graded bedding. *J. sedim. Petrol. 35*: 956–63.

RIEDEL, W. R. and FUNNELL, B. M. 1964: Tertiary sediment cores and microfossils from the Pacific Ocean floor. *Q. Jl geol. Soc. Lond. 120*: 305–68.

RITTENBURG, S. C., EMERY, K. O., HULSEMANN, J., DEGENS, E. T., FAY, R. C., REUTER, J. H., GRADY, J. R., RICHARDSON, S. H., and BRAY, E. E., 1963: Biogeochemistry of sediments from the experimental Mohole. *J. sedim. Petrol. 33*: 140–72.

RYAN, W. B. F. and HEEZEN, B. C. 1965: Ionian Sea submarine canyons and the 1908 Messina turbidity current. *Bull. geol. Soc. Am. 76*: 915–32.

SCHAEFER, W. 1962: "Aktuo-Palaeontologie". Verlag Waldemar Kramer, Frankfurt am Main.

SHEPARD, F. P. 1956: Marginal sediments of Mississippi Delta. *Bull. Am. Ass. Petrol. Geol. 40*: 2537–623.

——— 1958: Sedimentation of the northwestern Gulf of Mexico. *Geol. Rdsch. 47*: 150–67.

——— 1963: "Submarine Geology". 2nd ed. Harper and Row, New York.

SHEPARD, F. P. and EINSELE, G. 1962: Sedimentation in San Diego Trough and contributing submarine canyons. *Sedimentology 1*: 81–133.

SMITH, A. J. 1959: Structures in the stratified Late-Glacial clays of Windermere, England. *J. sedim. Petrol. 29*: 447–53.

TAYLOR, D. W. 1948: "Fundamentals of Soil Mechanics." John Wiley, New York.

VAN STRAATEN, L. M. J. U. 1959: Minor structures of some Recent littoral and neritic sediments. *Geologie Mijnb. N. F. 21*: 197–216.

WOOD, A. and SMITH, A. J. 1958: The sedimentation and the sedimentary history of the Aberystwyth Grits (Upper Llandoverian). *Q. Jl geol. Soc. Lond. 114*: 163–95.

INDEX

MEMOIRS OF THE NEW ZEALAND OCEANOGRAPHIC INSTITUTE

obtainable from the Publications Officer, Information Service, DSIR, Private Bag, Wellington, New Zealand

The number in square brackets for each Memoir is the N.Z. DSIR Bulletin Series number

1 Bibliography of New Zealand Oceanography, 1949-1953. N.Z. OCEANOGRAPHIC COMMITTEE. [N.Z. DSIR Geophysical Memoir 4] 1955

2 General Account of the Chatham Islands 1954 Expedition. By G. A. KNOX [122] 1957

3 Contributions to Marine Microbiology. Compiled by T. M. SKERMAN [N.Z. DSIR Information Series 22] 1959

4 Biological Results of the Chatham Islands 1954 Expedition. Part I. Decapoda Brachyura, by R. K. DELL; Cumacea, by N. S. JONES; Decapoda Natantia, by J. C. YALDWYN [139(1)] 1960

5 Biological Results of the Chatham Islands 1954 Expedition. Part 2. Archibenthal and Littoral Echinoderms. By H. BARRACLOUGH FELL [139(2)] 1960

6 Biological Results of the Chatham Islands 1954 Expedition. Part 3. Polychaeta Errantia. By G. A. KNOX [139(3)] 1960

7 Biological Results of the Chatham Islands 1954 Expedition. Part 4. Marine Mollusca, by R. K. DELL; Sipunculids, by S. J. EDMONDS [139(4)] 1960

8 Hydrology of New Zealand Coastal Waters, 1955. By D. M. GARNER [138] 1961

9 Analysis of Hydrological Observations in the New Zealand Region, 1874–1955. By D. M. GARNER [144] 1962

10 Hydrology of Circumpolar Waters South of New Zealand. By R. W. BURLING [143] 1961

11 Bathymetry of the New Zealand Region. By J. W. BRODIE [161] 1964

12 Hydrology of New Zealand Offshore Waters. By D. M. GARNER and N. M. RIDGWAY [162] 1965

13 Biological Results of the Chatham Islands 1954 Expedition. Part 5. Porifera: Demospongiae, by PATRICIA R. BERGQUIST; Porifera: Keratosa, by PATRICIA R. BERGQUIST; Crustacea Isopoda: Bopyridae, by RICHARD B. PIKE; Crustacea Isopoda: Serolidae, by D. E. HURLEY; Hydroida, by PATRICIA M. RALPH [139(5)] 1961

14 Submarine Morphology East of the North Island, New Zealand. By H. M. PANTIN [149] 1963

15 Marine Geology of Cook Strait. By J. W. BRODIE [in prep.]

16 Bibliography of New Zealand Marine Zoology 1769–1899. By DOROTHY FREED [148] 1963

17 Studies of a Southern Fiord. By T. M. SKERMAN (Ed.) [157] 1965

18 The Fauna of the Ross Sea. Part 1. Ophiuroidea. By H. BARRACLOUGH FELL [142] 1961

19 The Fauna of the Ross Sea. Part 2. Scleractinian Corals. By DONALD F. SQUIRES [147] 1962

20 *Flabellum rubrum* (Quoy and Gaimard). By DONALD F. SQUIRES [154] 1963

21 The Fauna of the Ross Sea. Part 3. Asteroidea. By HELEN E. SHEARBURN CLARK [151] 1963

22 The Marine Fauna of New Zealand: Crustacea Brachyura. By E. W. BENNETT [153] 1964

23 The Marine Fauna of New Zealand: Crustaceans of the Order Cumacea. By N. S. JONES [152] 1963

24 A Bibliography of the Oceanography of the Tasman and Coral Seas, 1860–1960. By BETTY N. KREBS [156] 1964

25 A Foraminiferal Fauna from the Western Continental Shelf, North Island, New Zealand. By R. H. HEDLEY, C. M. HURDLE, and I. D. J. BURDETT [163] 1965

26 Sediments of Chatham Rise. By ROBERT M. NORRIS. [159] 1964

27 The Fauna of the Ross Sea. Part 4. Mysidacea. By OLIVE S. TATTERSALL. Part 5. Sipunculoidea. By S. J. EDMONDS [167] 1965

28 Sedimentation in Hawke Bay. By H. M. PANTIN [171] 1966

29 Biological Results of the Chatham Islands 1954 Expedition. Part 6. Scleractinia, by D. F. SQUIRES. [139(6)] 1964

30 Geology and Geomagnetism of the Bounty Region east of the South Island, New Zealand. By D. C. KRAUSE [170] 1966

31 Contributions to the Natural History of Manihiki Atoll, Cook Islands. Compiled by C. MCCANN and J. S. BULLIVANT [In press]

32 The Fauna of the Ross Sea. Part 5. General Accounts, Station Lists, and Benthic Ecology. By John S. BULLIVANT and JOHN H. DEARBORN [176] 1967

33 The Submarine Geology of Foveaux Strait. By D. J. CULLEN [184] 1967

34 Benthic Ecology of Foveaux Strait. By E. W. DAWSON [In prep.]

35 The Marine Fauna of New Zealand: Spider Crabs, Family Majidae (Crustacea Brachyura). By D. J. GRIFFIN [172] 1966

36 Water Masses and Fronts in the Southern Ocean south of New Zealand. By TH. J. HOUTMAN [174] 1967

37 The Marine Fauna of New Zealand: Porifera, Demospongiae. Part I. Tetractinomorpha and Lithistida. By PATRICIA R. BERGQUIST [188] 1968

38 The Marine Fauna of New Zealand: Intertidal Foraminifera of the *Corallina officinalis* zone. By R. H. HEDLEY, C. M. HURDLE, and I. D. J. BURDETT [180] 1967

39 Hydrology of the Southern Hikurangi Trench Region. By D. M. GARNER [177] 1967

40 Sediments of the Western Shelf, North Island, New Zealand. By J. C. MCDOUGALL and J. W. BRODIE [179] 1967

41 Bathymetry and Geological Structure of the North-western Tasman Sea-Coral Sea-South Solomon area of the South-western Pacific Ocean. By DALE C. KRAUSE [183] 1967

42 The Echinozoan Fauna of the New Zealand Subantarctic Islands, Macquarie Island, and the Chatham Rise. By D. L. PAWSON [187] 1968

43 The Marine Fauna of New Zealand: Scleractinian Corals. By D. F. SQUIRES and I. W. KEYES [185] 1967

44 A Checklist of Recent New Zealand Foraminifera. By J. V. EADE [182] 1967

45 A Key to the Recent Genera of the Foraminiferida. By K. B. LEWIS [196] 1970

46 The Fauna of the Ross Sea. Part 6. Ecology and Distribution of Foraminifera. By J. P. KENNETT [186] 1968

47 An Outline Distribution of the New Zealand Shelf Fauna. Benthos Survey and Station List; Distribution of the Echinoidea. By D. G. MCKNIGHT [195] 1969

48 Hydrology of the South-east Tasman Sea. By D. M. GARNER [181] 1967

49 The Fauna of the Ross Sea. Part 7: Pycnogonida: Colossendeidae, Pycnogonidae, Endeidae, and Ammotheidae. By W. F. FRY and J. W. HEDGPETH [198] 1969

50 The Marine Geology of the New Zealand Subantarctic Seafloor. By C. P. SUMMERHAYES [190] 1969

51 The Marine Fauna of New Zealand: Porifera. Demospongiae. Part 2: Axinellidae and Halichondrida. By PATRICIA R. BERGQUIST [197] 1970

52 The Marine Fauna of New Zealand: Sea Cucumbers (Echinodermata: Holothuroidea). By D. L. PAWSON [201] 1970

53 Zooplankton and Hydrology of Hauraki Gulf, New Zealand. By J. B. JILLETT [204] 1971

54 Systematics and Ecology of New Zealand Central East Coast Plankton sampled at Kaikoura. By J. M. BRADFORD [207] 1972

55 Bay Head Sand Beaches of Banks Peninsula, New Zealand. By P. R. DINGWALL [In prep.]

56 Hydrology of the Southern Kermadec Trench Region. By N. M. RIDGWAY [205] 1970

57 Biological Results of the Chatham Islands 1954 Expedition. Part 7. Bryozoa Cheilostomata. By G. H. UTTLEY and J. S. BULLIVANT [139(7)] 1972

58 Hydrological Studies in the N.Z. Region 1966 and 1967. Oceanic Hydrology North-west of N.Z., Hydrology of the North-east Tasman Sea. By D. M. GARNER [202] 1970

59 The Fauna of the Ross Sea. Part 8: Pelagic Copepoda by JANET M. BRADFORD, Cumacea by N. S. JONES [206] 1971

A. R. SHEARER, GOVERNMENT PRINTER, WELLINGTON, NEW ZEALAND—1972

79117A—1,520/6/70 A